IDENTIFICATION AND CHARACTERIZATION OF NATURAL FRACTURES WHILE DRILLING UNDERBALANCED

by

Jack H. Norbeck

A thesis submitted to the Faculty and the Board of Trustees of the Colorado School of Mines in partial fulfillment of the requirements for the degree of Master of Science (Engineering).

Golden, Colorado

Date _____

Signed: _____
Jack Norbeck

Signed: _____
Dr. D.V. Griffiths
Thesis Advisor

Golden, Colorado

Date _____

Signed: _____
Dr. Kevin Moore
Professor and Dean
Department of Engineering

ABSTRACT

This thesis describes an algorithm based on data obtained during underbalanced drilling operations to identify the location and properties of productive natural fractures that are intersected by the wellbore. Fluid production during the drilling process provides the basis for locating conductive natural fracture zones along the wellbore. In addition, an approach is described for estimating the permeability of each conductive feature. A validation technique is employed in order to quantify the level of confidence in the proposed methodologies.

The methodologies developed in this report are applied to drilling and mud log data from six horizontal wells in tight gas reservoirs that were drilled underbalanced. Conductive natural fracture zones are determined through a screening process using a set of fracture identification criteria. The permeability of each fracture zone is then calculated using estimates of gas influx rate. The wells investigated consist of three sets of parallel wells with horizontal spacing of roughly 700 ft. The results from the natural fracture characterization analysis for each pair of wells are compared. It is argued that patterns in the locations of conductive natural fractures in parallel wells could be an indication of the orientation of the natural fracture system in the region.

In two of the three well pairs considered, the majority of identified conductive fracture locations in one well aligned with a corresponding feature in the parallel well. The confidence level in these methodologies is moderate to high.

The flow contribution from natural fractures is known to dominate production from tight gas reservoirs, however, gaining information about the geometry and permeability of the natural fracture system is often impossible or cost prohibitive. The methodologies described in this thesis make use of data that is commonly recorded for virtually every new well that is drilled, reducing the need to contract expensive image log tests. Additionally, the methodologies can be applied in near real-time as the well is drilled. The information obtained from this type of natural fracture characterization analysis can be used to improve hydraulic fracture treatment designs.

TABLE OF CONTENTS

LIST OF FIGURES

LIST OF TABLES

ACKNOWLEDGEMENTS

First and foremost, I would like to thank all of my loving family members and friends for standing strong behind me throughout my entire life, but especially over the duration of this work. Your endless support and encouragement never fails to give me strength when I need it most.

I will always be indebted to my thesis advisor, Dr. D.V. Griffiths. I will never forget that you were the first to notice my potential and give me the opportunity to achieve great things – working alongside you has truly been a great honor. My gratitude goes out to Dr. Azra Tutuncu and Dr. Marte Gutierrez for all of the sound advice you have provided over the last year.

Finally, I would like to thank Mr. Ernesto Fonseca, Mr. Mauricio Farinas, Dr. Sau-Wai Wong, and the rest of the Unconventional Gas R&D team at Shell for providing many intellectual contributions to this work. This thesis would not have been possible without your dedication to assist me and your confidence in my abilities.

The financial support of Shell International Exploration and Production Inc. is gratefully acknowledged.

CHAPTER 1: INTRODUCTION

As a result of the decline in gas reserves worldwide and an increase in energy consumption, the oil and gas industry has recently experienced a dramatic shift towards the development of reservoirs of extremely low permeability previously considered uneconomic (Stewart 1970; Vairogs et al. 1971; Agarwal et al. 1979). It is recognized that the development of these tight gas resources will play a key role in attaining energy security for the future. Currently, many of the largest known natural gas reservoirs, especially in North America, are considered low-permeability, or tight gas, reservoirs (see **Figure 1.1**). As illustrated in **Figure 1.2**, North America is estimated to hold over a quarter of the world's natural gas resource. Effectively tapping into these reserves will undoubtedly help to reduce the U.S.'s foreign oil and gas imports.

Additionally, with the recent concerns regarding climate change as a response to carbon dioxide emissions, natural gas presents a great opportunity to establish a precedence to promote low CO_2 emissions. As indicated by **Table 1.1**, burning natural gas produces roughly two-thirds the amount of CO_2 as oil and nearly half the amount of CO_2 as coal (Moore 2010).

In order to stimulate extensive production of tight gas reserves, new techniques for analyzing the long-term production capabilities of the wells must be implemented. Although the preferred method is production data analysis, there are many limitations encountered when attempting to apply these techniques to tight gas reservoirs. Most notably, it has often been reported that tight gas wells require economically prohibitive shut-in times, on the order of months, before the data can be used for decline curve analysis and type curve matching (Anderson et al. 2010). Additionally, engineers have realized that in order for tight gas reservoirs to be considered economic, vast fracture networks must be present. Both natural and hydraulic fractures have large impacts on production performance analysis of tight gas reservoirs. In a conventional reservoir, perhaps the most influential reservoir property on the performance of a well is the reservoir permeability. Permeability is a measure of how efficiently a rock can transmit fluids, typically measured in darcies or millidarcies. However, in a tight gas reservoir there is an intense interaction between the fractures that intersect the well and the intact formation (Wei and Economides 2005). The number of fractures in a formation and their connectivity, as well as the fracture characteristics, will have a large impact on the overall productivity of a well.

Characterization of the individual natural fractures and fracture networks has been recognized to be an extremely important factor for determining hydraulic fracturing procedures, well completion strategies, and estimating well performance (Aguilera 2008). There are currently

many well-testing methods used to deduce fracture properties including use of production data, core analyses, acoustic and resistivity image logs, and, most recently, use of drilling data. Any data that the engineer can obtain that will help to infer fracture properties such as fracture width fracture length, fracture permeability, fracture conductivity, and fracture orientation can have significant economic implications.

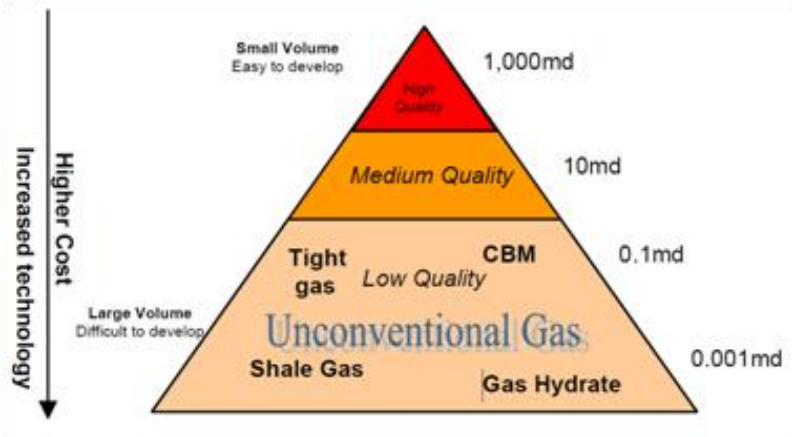

Figure 1.1 Cartoon illustrating the principle of unconventional gas resources. Globally, large quantities of natural gas exist in low permeability reservoirs. Technical and economic limitations impede progress in the development of these substantial resources. (Xiong and Holditch 2006).

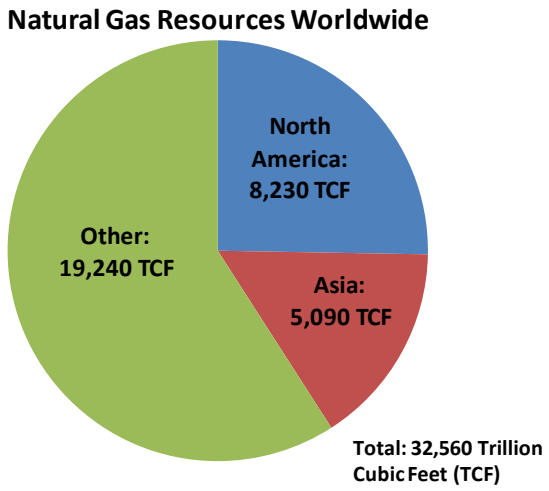

Figure 1.2 Chart illustrating the estimated worldwide distribution of natural gas resources. Over a quarter of the world's natural gas resource exists in North America. (Xiong and Holditch 2006).

Table 1.1 Table portraying the emission levels of various pollutants for natural gas, oil, and coal. Natural gas is considered a "clean" burning fossil fuel source with roughly half the CO2 emissions as coal. Note that burning natural gas produces zero mercury emissions. (Moore 2010).

Fossil Fuel Emission Levels
in Pounds per Billion Btu of Energy Input

Pollutant	Natural Gas	Oil	Coal
Carbon Dioxide	117,000	164,000	208,000
Carbon Monoxide	40	33	208
Nitrogen Oxides	92	448	457
Sulfur Dioxide	1	1,122	2,591
Particulates	7	84	2,744
Mercury	0.000	0.007	0.016

1.1 Motivations for Research and Problem Statement

The economic viability of a well drilled in an unconventional gas reservoir is largely influenced by the level of connectivity between natural fractures, stimulated fractures, and the wellbore. Engineers have the ability to control the wellbore path and, to some extent, the hydraulic fracturing process. On the other hand, natural fracture systems are outside of the engineer's control. While knowledge of the geologic conditions and stress history are helpful to estimate the characteristics of the natural fracture system in a given reservoir, the true extent of the natural fracture system in any specific location is typically unknown (i.e., near wellbore). Several well testing methods are available to the industry to identify natural fractures near the wellbore, including acoustic and resistivity image logs, but the poor-quality results of these techniques do not compensate for the expensive costs in most cases. The desire to learn as much as possible about the natural fracture systems present in tight gas plays while striving to keep drilling and completions costs to a minimum has led researchers to explore the use of drilling data as a means for natural fracture characterization.

Several reports in the literature indicate that it is possible to locate and characterize the permeability of natural fractures intersected by the drillbit during conventional, overbalanced drilling operations through the use of mud loss data. However, most wells in unconventional gas reservoirs are drilled underbalanced. For the case of underbalanced drilling, the downhole pressure condition requires that an alternate approach for natural fracture characterization be developed.

The investigation discussed within this thesis is essentially an exploitation study to determine whether valuable information concerning natural fracture systems that intersect horizontal wellbores in tight gas reservoirs can be discovered through the use of underbalanced drilling data. Methodologies are developed to determine highly probable conductive natural

fracture "zones" and, hence, characterize natural fracture permeability at these locations. The methods make use only of data that is commonly recorded by drilling engineers in practice during underbalanced drilling operations. The ability to apply the methods in a practical manner is facilitated by the development of a computational tool. Due to the high level of uncertainty inherent to this type of analysis, several practical validation analyses are identified and subsequently performed.

1.2 Background Material

In order to develop methodologies to use underbalanced drilling (UBD) data to locate and characterize the permeability of natural fractures which intersect the wellbore, it is necessary to introduce some relevant background material. First, it is essential to understand the current practice by which reservoir engineers are able to characterize reservoir and fracture properties. Special attention will be paid to the limitations of these conventional approaches when applied towards tight gas reservoirs. Second, an overview of the types of data collected during the drilling process will be discussed. Several categories of data that have potential to be indicators of the presence of natural fractures will be identified. Third, fundamentals of gas flow through porous and fractured media will be described. Specifically, flow of gas through tight formations where permeability is less than 0.1 md and gas flow through fractures will be reviewed to provide a basis for characterization of natural fracture permeability.

1.2.1 Reservoir Characterization

Production data analysis (PDA) is the most common technique used to evaluate production performance of wells by providing estimates of reservoir permeability, fracture length, fracture conductivity, well drainage area, original gas in place (OGIP), estimated ultimate recovery (EUR), and skin effects. The advantage of PDA is that production rate and cumulative production data are two pieces of information that are recorded for every well. A disadvantage to this method is that it can often take years to obtain the necessary data. Many different PDA methods have been proposed, but no single approach has been proven to always give the most accurate results (Gaskari et al. 2006). All available methods can be categorized into one of two subsets of PDA techniques: decline-curve analysis (DCA) or type-curve matching (TCM).

The first DCA approach was proposed by Arps (1945) and was based purely on an empirical extrapolation of production rate data. The relationship between production rate and time is illustrated by the following equation representing a declining trend (Arps 1945):

$$\dot{q}(t) = \frac{\dot{q}_i}{(1 + bD_i t)^{1/b}} \tag{1.1}$$

Here $\dot{q}(t)$ is the oil or gas production rate at time t, $\dot{q}_i$ is the initial production rate, and b and D_i are two constants. For the two special cases of $b = 0$ and $b = 1$, Equation 1.1 will take the following forms, respectively:

$$\dot{q}(t) = \dot{q}_i e^{-D_i t} \tag{1.2}$$

$$\dot{q}(t) = \frac{\dot{q}_i}{(1 + D_i t)} \tag{1.3}$$

Equation 1.2 represents production rate data that exhibits an exponential decline, whereas Equation 1.3 represents production rate data that exhibits a harmonic decline. Any values of b between 0 and 1 represent a hyperbolic decline of production rate.

Production rate can also be shown to be a function of cumulative production. For the example of exponential decline:

$$q(t) = \int_0^t \dot{q}(t)dt = \int_0^t \dot{q}_i e^{-D_i t} dt \tag{1.4}$$

Here $q(t)$ represents cumulative production as a function of time. Solving Equation 1.4 yields:

$$q(t) = -\frac{1}{D_i}(\dot{q}_i e^{-D_i t}) + \frac{\dot{q}_i}{D_i} \tag{1.5}$$

Combining Equations 1.2 and 1.5, and rearranging for production rate, $\dot{q}(t)$, results in:

$$\dot{q}(t) = -D_i q(t) + \dot{q}_i \tag{1.6}$$

Similar results can be obtained for the harmonic and hyperbolic cases. The results indicate that plots of rate vs. time and rate vs. cumulative production are both useful for determining the correct values of D_i and b for a given well.

In general, it is difficult to predict which behavior a particular reservoir will exhibit. Type-curves can be generated for the empirical Arps (1945) equation based on different values of

b ranging between 0 and 1. Using records of production rate and cumulative production, field data can be plotted over the type-curves, and the resulting match will provide a good estimate of the values for D_i and b. The power behind the DCA method is that once the correct match has been determined for a given well, the trend can then be extrapolated to a specific time in the future to estimate ultimate recoveries. **Figures 1.3a-d** illustrate examples of shapes of rate vs. time and rate vs. cumulative production curves exhibiting the three types of behavior. Additionally, making use of properties of logarithms further enhances the ability of the engineer attempting to match the correct parameters for a well. Depending on the type of plot and the type of behavior, when plotted on a semilog scale some trends will appear linear which can make it easier to determine the behavior of field data.

Lee and Wattenbarger (1996) remind users of PDA methods that Equation 1.1 is based on four important and widely violated assumptions.

1. The equation assumes that the well analyzed is produced at *constant* BHP [bottomhole pressure]. If the BHP changes, the character of the well's decline changes.
2. It assumes that the well analyzed is producing from an unchanging drainage area (i.e., fixed size) with *no-flow boundaries*.
3. The equation assumes that the well analyzed has constant permeability and skin factor. If permeability decreases as pore pressure decreases, or if skin factor changes because of changing damage or deliberate stimulation, the character of the well's decline changes.
4. It must be applied *only* to boundary-dominated (stabilized) flow data if we want to predict future performance of even limited duration. If the data "fit" with a decline curve are transient, there is simply no basis for predicting long-term performance. Until *all* the boundaries of the drainage area (or reservoir) have influenced the well's decline characteristics, predictions of the long-term decline rate are not unique and, except by sheer accident, are incorrect," (Lee and Wattenbarger 1996).

It should be emphasized that the Arps (1945) DCA curves have no physical basis and rely on empirical trends. Because of this shortcoming, several publications have attempted to provide a theoretical basis for type-curves (e.g., Fetkovich 1980; Carter 1985; Cox et al. 1996). These sets of type-curves relate the production rate decline trend to practical engineering flow parameters and are based on theoretical solutions to flow equations.

Although PDA techniques have been an extremely useful tool for reservoir characterization, they have been developed mostly for conventional reservoirs and vertical well

systems. Application of these techniques towards tight gas reservoirs results in numerous problems. Most TCM techniques are based on the assumption that the reservoir exhibits radial flow. This implies that flow is converging towards the wellbore in all directions. However, analysis of decline curves for tight gas wells has suggested that these reservoirs can often exhibit linear flow for over 10 or 20 years, never reaching radial flow throughout the entire productive life of the well (Millheim and Cichowicz 1968; Wattenbarger et al. 1998). Linear flow, which is characterized by flow paths that act parallel to each other, is thought to be caused by presence of fractures (see **Figure 1.4a**). In addition, conventional type-curve methods only allow for the interpretation that linear flow is the result of a single fracture associated with the well (Anderson et al. 2010). Tight gas reservoirs are commonly completed with a horizontal well that intersects multiple transverse fractures. Conventional PDA methods cannot account for the complexity of this occurrence. In an attempt to overcome the restraints of the conventional models, several publications have proposed DCA/TCM techniques that are directly applicable to extremely low-permeability and highly fractured formations (e.g., Wattenbarger et al. 1998; Anderson et al. 2010). Regardless, the PDA methods are somewhat limited for application in tight gas reservoirs, and more advanced techniques must be developed to characterize the natural and stimulated fracture systems.

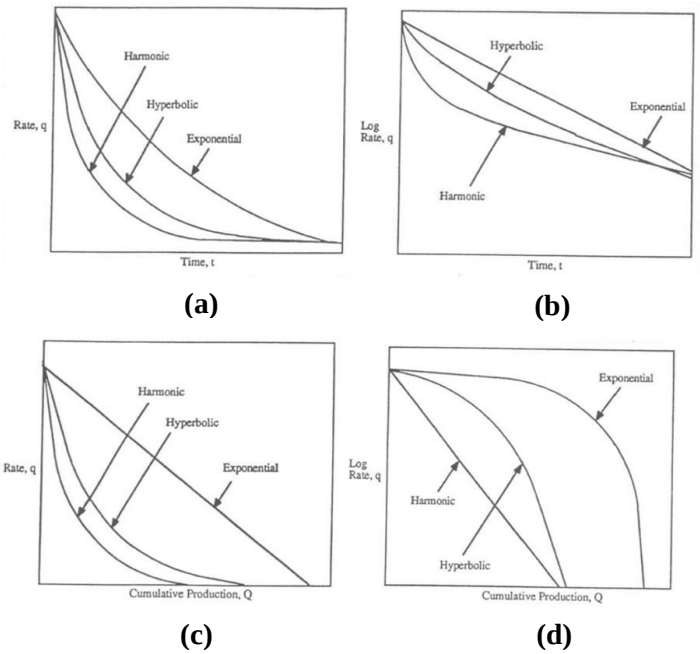

Figure 1.3 These charts are generalized plots of production rate, $\dot{q}$, and cumulative production, q, versus time. Both Cartesian plots and semi-log plots are shown. (Lee and Wattenbarger 1996).

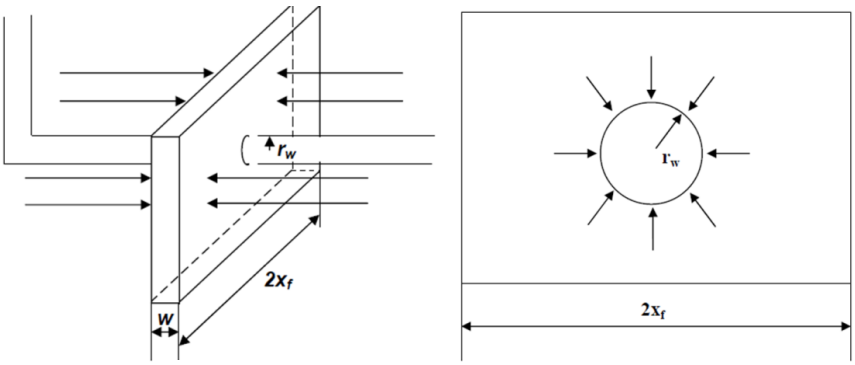

(a) **(b)**

Figure 1.4 a) Flow from the formation into the fracture is linear followed by **b)** converging radial flow within the fracture. These flow patterns are the most common assumptions for fluid flow models (Wei and Economides 2005).

1.2.2 Overview of Drilling Data

At least two data sets are almost universally generated while drilling an oil or gas well. The first is called the drilling log. This provides measurements that are critical to evaluating the overall drilling process. The drilling log contains information about the progress of the well such as measured depth (MD), true vertical depth (TVD), inclination, weight on bit (WOB), rate of penetration (ROP), and gamma ray. It also provides information about the drilling mud circulation system such as mud pit volume, pump pressure, and mud flow rate. This type of data can be used for QA/QC purposes as the well is drilled.

The second data set is called the mud log. This log is generally created by the on-site geologist as the well is drilled. Many things can be recorded in the mud log depending on the contractor, but two features should exist in all mud logs: formation geology and total gas measurements. As the drillbit penetrates the formation the rock is crushed, and these cuttings are flushed from the well and carried to the surface by the circulating drilling mud. A geologist will examine the cuttings and inform the drilling engineer which type of formation is currently being penetrated. This information is recorded in the mud log on a depth basis as the well is drilled in order to create a geologic profile of the entire well. However, for the purposes of this study, the total gas measurements are far more interesting and useful.

Total gas measurements indicate the relative concentration of hydrocarbons (methane, ethane, propane, etc.) present in the circulating drilling mud at any given time. In general, there will be gasses entrained within the drilling mud as a response to the following four scenarios (Mercer 1974). *Liberated* fluids occur when gas that is originally trapped within the pore spaces of the formation rock is released into the drilling mud as the drillbit crushes the rock. Liberated

fluids will be an indicator of the type of hydrocarbon contained in the rock at the time of drilling. *Produced* fluids will enter the circulating drilling mud in the case that the reservoir pore pressure exceeds the downhole pressure. During conventional drilling operations the drilling mud density is maintained above the reservoir pore pressure for wellbore stability issues. As such, produced fluids can only occur when an unexpected overpressured zone is encountered or when a transient mud pressure reduction occurs as the drillstring is raised (swabbing). Recent innovations in drilling techniques have led to the development of underbalanced drilling, in which the circulating mud pressure is deliberately maintained below the reservoir pore pressure throughout the drilling process. In this case, hydrocarbon production will occur consistently during drilling, especially as a high permeability zone is intersected (e.g., natural fracture). Produced fluid as a result of the underbalanced pressure condition is a major focus of this investigation. *Recycled* fluids may occur if the gas contained within the circulating mud is not entirely released at the surface. In this instance, the remaining gas will be re-circulated through the system and will be detected again on the next pass. Finally, *contamination* will always occur due to various unavoidable causes. Reasons for contamination of the total gas readings include petroleum products intentionally added to the drilling mud, chemical reactions and degradation of organic mud additives, and even emissions from construction equipment on-site. It is very important to understand all of these processes so that one can effectively interpret the mud log analysis.

The drilling fluid circulation system is essentially a closed loop system in which the mud is pumped down the well through the center of the drillstring, flows through the drillbit nozzle, and is then forced back up to the surface through the annular section. This process ensures that the drillbit stays cool, creates a hydrostatic pressure that is exerted against the wellbore wall for well stability issues, and flushes the cuttings to the surface. At the surface, the mud is transported through a shaker table to remove the cuttings and then released into a mud pit to complete the cycle.

To obtain the total gas measurements a gas trap is installed at the mud pit that is able to capture a sample of gas from the mud. **Figure 1.5** illustrates the concept of a gas trap. An impeller agitates the mud releasing gas into the air. A mixture of this gas-air sample is then sent to the mud logging unit for analysis. The total gas reading is a measure of the relative concentration of all hydrocarbons combined. The unit of measurement for total gas is simply called a "unit." Each contractor has their own definition of a unit, but, regardless of the conversion factor, the unit is effectively a concentration (i.e., ppm). The total gas measurements are recorded on a time basis and then converted to a depth basis through knowledge of the ROP.

It is then corrected to account for the lag time, which is the time it takes the drilling mud to travel from the bottomhole to the surface.

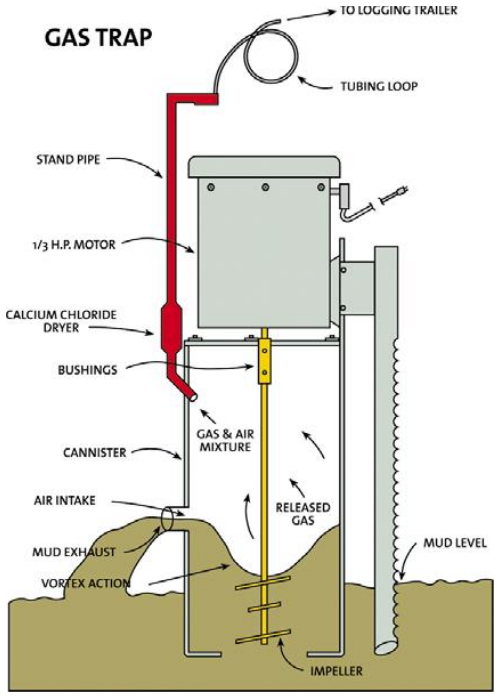

Figure 1.5 Illustration of the gas trap system. The stream of circulating drilling mud enters the gas trap where an impeller agitates the mud, releasing trapped gasses into the air. A portion of this gas-air sample is pumped to the gas logging unit where the total gas measurements are recorded. (Geosearch Logging Inc.).

Conventionally, the total gas readings have two main purposes. An obvious application of the mud log is that total gas "shows" help to delineate productive, hydrocarbon rich zones along the wellbore. Completion engineers will use this information to design effective completion strategies in order to maximize production. The second purpose is perhaps the more critical application. Total gas measurements can provide a means for the early detection of large gas kicks that can threaten to blow out a well. The drilling engineer will usually adjust the density of the drilling mud to overcome the formation pore pressure. A gas kick is a dangerous situation that can occur if the well intercepts an unexpected overpressured zone. A gas kick implies that a large gas bubble has entered the annular section of the wellbore and may or may not be rapidly rising towards the surface. "Loss of well control during drilling operations constitutes one of the major hazards faced by rig personnel, and can lead to loss of life and major destruction of a drilling installation," (Wang et al. 1994). **Figure 1.6** illustrates the importance of the mud log data. The picture shows a flare from a zone that was previously unknown to contain hydrocarbons and exhibited no change in drilling characteristics. However, the mud logging unit

detected a large presence of gas in the drilling fluid and the drilling engineer and company man were immediately notified. The well was controlled and the gas was flared with no impact to the safety of the crew.

Figure 1.6 Photograph of a gas flare. The mud log indicated that the well had taken a dangerous kick and the well was subsequently controlled. (Geosearch Logging Inc.).

Interpretation of the mud log requires a deep understanding of the fundamental processes that that contribute to the recorded total gas measurements. Many considerations must be accounted for if the mud log is to provide meaningful information. The present study is heavily reliant upon high quality mud log interpretations so the following example of a mud log analysis is well deserved.

The example shown in **Figure 1.7** represents an ideal mud log report. This particular mud log contains measurements or estimates of ROP, mud density (mud weight), static and circulating mud pressure, reservoir pore pressure, and total gas. Additionally, it is observed that information regarding the points at which drillstring connections were made is reported. In fact, knowledge of the measured depth locations of where the connections are made is one of the most critical pieces of data necessary to perform a mud log analysis, especially for the purposes of this study. As a drillstring connection is made the circulation of drilling fluid is halted. During the time it takes to make the connection any produced or liberated fluids will accumulate at the bottom of the well. Once the drilling mud returns to circulation, this gas will cause an artificially high total gas peak on the mud log. This process is called a connection gas event. Another common event is called trip gas, which occurs whenever a trip is performed. These events are manifestations of the drilling operation and must not be mistaken as responses to reservoir conditions.

In **Figure 1.7**, the first appearance of a total gas reading is due to a connection gas event at the point when the formation pore pressure begins to exceed the static mud pressure. Once the formation pore pressure becomes greater than the circulating mud pressure, a true gas show is observed. The drilling engineer understands that this gas show is a result of the mud density being too low, and the decision is made to increase the mud density. Subsequently, both the static and circulating mud pressure exceed the formation pore pressure, suppressing any gas entry into the wellbore.

This idealized case is relatively straightforward, however, in practice the task of interpreting the mud log can be much more difficult. For instance, the true formation pore pressure gradient is usually unknown, and an empirical estimate is often the best available information. In many cases, the information regarding drillstring connections is not appropriately labeled on the mud log. Additionally, the total gas measurements are never as clear as is indicated in **Figure 1.7**, and in reality are quite noisy.

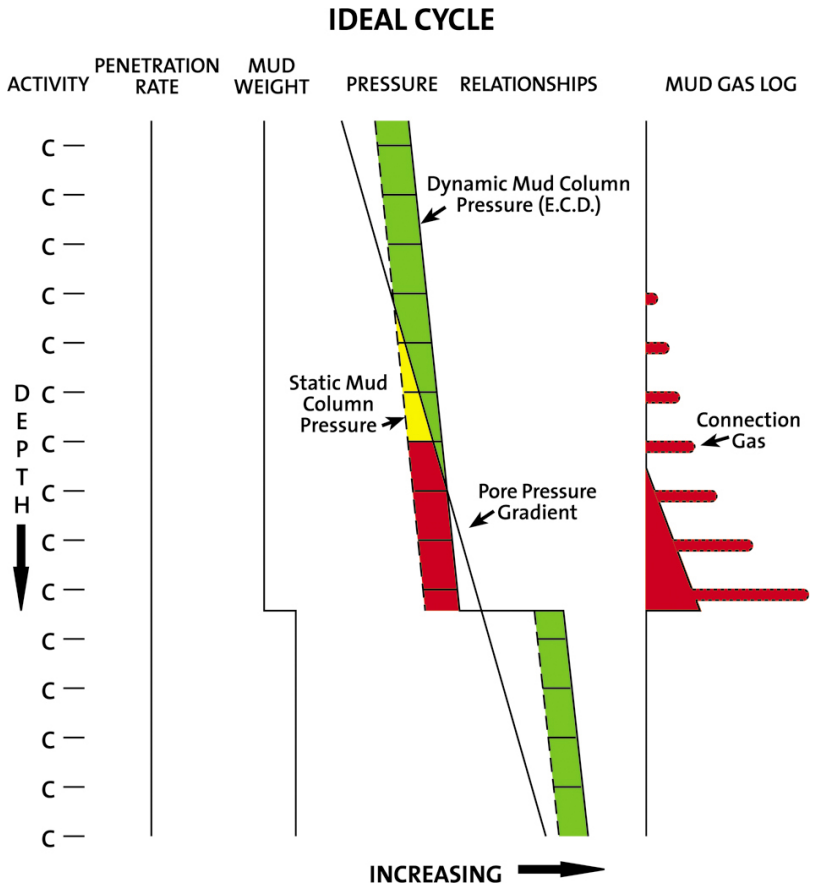

Figure 1.7 Depiction of an idealized mud log report. This diagram is helpful for understanding how to interpret gas shows observed on the mud log. (Geosearch Logging Inc.).

The focus of this study is on tight gas shale reservoirs with matrix permeability less than 0.1 md. These reservoirs are known to contain a high density of natural fractures and production is in fact dominated by fracture flow. Typically, it is presumed that vertical natural fractures exist in-situ. Therefore, to produce economically from these types of reservoirs it is most efficient to drill horizontal wellbores. The lateral sections of these wellbores are often drilled underbalanced. During underbalanced drilling operations, gas is expected to flow into the wellbore consistently throughout the drilling process. The combination of low permeability matrix, high permeability natural fractures, and the underbalanced pressure condition leads to the result of highly complicated mud logs. However, a thorough analysis of the mud log data can reveal critical information about the natural fracture system near the wellbore.

1.2.3 Gas Flow through Porous and Fractured Media

A large focus of the present study is on characterization of the permeability of natural fractures that intersect horizontal wellbores. It is necessary to have a fundamental understanding of the methods used to model gas flow through porous media and fractures. Special attention will be paid to highly fractured natural gas reservoirs with extremely low matrix permeability. First, gas flow at the reservoir scale will be introduced. Then, gas flow through individual fractures will be discussed.

Fluid flow through a porous media is fundamentally governed by Darcy's law:

$$\vec{v} = -\frac{k}{\mu}\nabla P \tag{1.7}$$

Here $\vec{v}$ is fluid velocity, k is formation permeability, μ is fluid viscosity, and P is pressure. Formation permeability is an intrinsic property of the porous media that describes the ability or ease for fluid to flow through the media. In the context of petroleum engineering, permeability has units of area. Permeability is not to be confused with the term commonly called hydraulic conductivity in civil engineering, which has units of velocity. Hydraulic conductivity is specifically used for flow of water through porous media and is a property of both the porous media and the fluid. The following comparison illustrates the relationship between permeability, hydraulic conductivity, and water properties.

Consider Equation 1.7 rewritten in terms of fluid velocity in one dimension for simplicity:

$$v = -\frac{k}{\mu}\frac{\Delta P}{L} \tag{1.8}$$

where L is the sample length. This is the convention used commonly in petroleum engineering. Now consider the form used commonly in civil engineering applications:

$$v = -\kappa\frac{\Delta h}{L} \tag{1.9}$$

Here κ is hydraulic conductivity and h is hydraulic head. These two expressions effectively describe the same process, the difference in notation being that the petroleum engineering approach is in terms of a pressure drop and the civil engineering approach is in terms of a hydraulic head loss. In fact, the following relationship can be shown:

$$\Delta P = \rho g \Delta h \tag{1.10}$$

Substituting Equation 1.10 into 1.8 and equating Equations 1.8 and 1.9 gives the following:

$$-\frac{k}{\mu}\frac{\rho g \Delta h}{\Delta L} = -\kappa\frac{\Delta h}{\Delta L} \tag{1.11}$$

Rearranging Equation 1.11 to solve for hydraulic conductivity results in the following expression:

$$\kappa = k\frac{\rho g}{\mu} \tag{1.12}$$

From Equation 1.12 it is clear that the civil engineer's hydraulic conductivity is indeed related to the petroleum engineer's permeability. The distinction is that permeability is solely a property of the porous media, whereas hydraulic conductivity incorporates the permeability of the porous media as well as the properties of the fluid (e.g., water).

Most models used for characterizing fractured hydrocarbon reservoirs are based on pressure transient flow. Assuming Darcy flow, single phase, slightly compressible fluid flow through a porous medium can be expressed by the following diffusivity equation:

$$\frac{k}{\mu}\nabla^2 P = \phi c_t \frac{\partial P}{\partial t} \tag{1.13}$$

In this partial differential equation P is pressure, k is formation permeability, ϕ is formation porosity, μ is fluid viscosity, and c_t is total compressibility. The diffusivity equation assumes constant reservoir and fluid parameters. Equation 1.13 describes how fluid pressure within the formation varies both spatially and temporally. The diffusivity equation forms the basis for most reservoir simulation packages used throughout industry.

For gas reservoirs Equation 1.13 poses two major problems. The most obvious problem arises due to the high compressibility of gas and its variation of viscosity with changes in pressure. The second problem is that due to the low cross-sectional area of wellbores, velocities near the wellbore can become very high. Darcy's law states that the relationship between volumetric flow rate and pressure gradient is linear. At high velocities Darcy flow is not valid because of turbulent effects (Basquet et al. 2004). To account for non-Darcy flow, the Forchheimer equation is often used to describe turbulent behavior as follows (e.g., Zeng and Zhao 2010):

$$-\nabla P = \frac{\mu}{k} v + \rho \beta v^2 \tag{1.14}$$

Here ρ is the fluid density and β is an inertial factor and is a property of the porous media. The first term on the right hand side of Equation 1.14 represents viscous flow that is dominant at low velocities. The second term on the right hand side represents the additional pressure drop resulting from the friction or inertial effects during non-Darcy flow. Equation 1.14 indicates that at low velocities the second term is negligible, and the equation reduces to Darcy's law. At high velocities, the second term dominates and can substantially affect the pressure gradient. An alternate form of Equation 1.13 can be derived to include the Forchheimer equation.

Recent interest in unconventional reservoirs in which fluid flow is dominated by flow through a fracture network has led to development of analytical models and reservoir simulators that can handle the complex interaction between matrix rock and fractures. The double porosity approach was introduced by Warren and Root (1963) (see **Figure 1.8**). The approach operates on the concept that fractures have large permeability but low porosity as a fraction of the total pore volume. The matrix rock has the opposite properties: low permeability but relatively high porosity. This approach describes the observation that fluid flow will only occur through the fracture system on a global scale. Locally, fluid may flow between matrix and fractures through interporosity flow, driven by the pressure gradient between matrix and fractures.

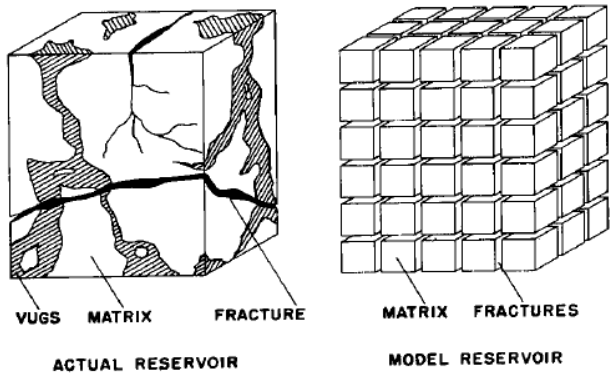

Figure 1.8 The classic Warren and Root dual porosity model. This model provides the basis for many fractured reservoir numerical simulation codes. (Warren and Root 1963).

Fluid flow within individual fractures is most commonly modeled through the cubic law relationship (Snow 1965):

$$\frac{Q}{\Delta P} = Cw^3 \tag{1.15}$$

Here Q is volumetric flow rate, P is pressure, C is a constant dependent on the type of flow, and w is fracture aperture. For radial flow, the value of C is given by the following equation (Witherspoon et al. 1979):

$$C = \left(\frac{1}{12\mu}\right)\left[\frac{2\pi}{\ln(R_e / R_w)}\right] \tag{1.16}$$

In this expression R_e / R_w is the ratio of the extent of the fracture to wellbore radius. The cubic law assumes steady-state, laminar flow between two parallel surfaces. The assumptions are not generally valid for the conditions observed in the present research, but in most practical research applications the cubic law is used to gain insight into fracture properties, even in transient analyses (Wu, personal communication).

Fracture permeability is defined in the same way that the formation permeability is defined, in that it is an intrinsic property of the medium that measures the ability for flow to occur through the fracture. Poiseuille's law indicates that fracture permeability depends on the width of the fracture (e.g., Chen et al. 2000):

$$k_f = \frac{w^2}{12} \tag{1.17}$$

Fracture geometries are often idealized to simplify modeling efforts. In most cases the width is assumed to be constant, and the fracture is usually considered either a perfect rectangle (e.g., Wei and Economides 2005) or a perfect circle (e.g., Huang et al. 2010). In reality, fracture geometries are very complex (**Figure 1.9**), and many different factors could affect the behavior of fluid flow (Mourzenko et al. 1995). For application in dynamic reservoir characterization using real-time mud log data, the term "sweet spot" is used when the drill bit intersects a transverse natural fracture. It is generally assumed that these sweet spots are natural fractures with idealized geometries.

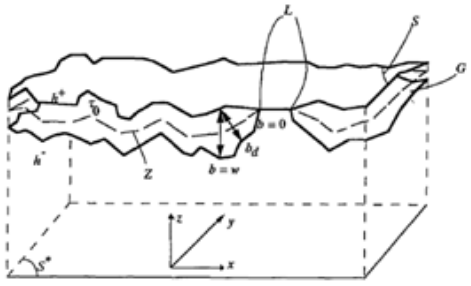

Figure 1.9 Illustration of a hypothetical fracture model developed to analyze the effects of fracture geometry on fluid flow through fractures. (Mourzenko et al. 1995).

CHAPTER 2: LITERATURE REVIEW

The topic discussed in this thesis brings together several areas of petroleum engineering, including drilling engineering, reservoir engineering, petrophysics, and production and completion engineering. An extensive literature review has been performed in order to understand previous work that has been published on issues related to natural fracture characterization and underbalanced drilling. First, the innovations that have made economic production from tight gas reservoirs will be addressed. Specifically, the ability to drill horizontal wells and then stimulate the lateral sections with massive hydraulic fracturing will be discussed. Second, conventional methods for characterizing the natural fracture system in these types of reservoirs will be investigated. These methods generally consist of image log techniques or core description. Third, recent efforts to make use of drilling data to enable "real-time" natural fracture and reservoir characterization are presented. These methods can be separated into two groups: those that use overbalanced drilling data and those that use underbalanced drilling data. It is observed that the topic addressed in the present research is a novel concept that has collected limited published material.

2.1 Advances in Tight Gas Exploration and Production

Increasing global energy demand requires developing innovative and cost effective drilling techniques and well completion strategies in order to efficiently access and produce from deep tight gas reserves. Significant progress has been made towards improving drilling methods since the 1990's. A key issue with respect to drilling in tight gas formations is that horizontal wells, rather than vertical wells, are often more likely to intersect the natural fractures that allow low-permeability zones to be considered productive (Woodrow et al. 2008). One technique that has been proven to effectively control a broad range of drilling uncertainties that come with drilling horizontal wells is termed managed pressure drilling (MPD). MPD uses tools at the surface such as a choke to control the drilling fluid flow rate and bottomhole pressure. The various drilling operations that MPD is comprised of provide economical solutions to many drilling problems such as: managing gas kicks, lost circulation and other well control issues, improving rate of penetration (ROP), minimizing formation damage, and enabling dynamic reservoir characterization from real-time mud log data (Ramalho et al. 2009). Underbalanced drilling (UBD) is a form of MPD that is particularly useful when drilling horizontal wells in tight gas formations (Ramalho 2006).

In addition to the ability to drill horizontal wells, advances in hydraulic fracturing techniques in the last few decades have drastically improved the ability to produce from unconventional reservoirs. Stimulated fractures create a pathway between the natural fracture system and the wellbore, allowing fluids to be produced at much larger capacities than in the natural state. The effects of hydraulic fracture treatments on overall well productivity will be discussed briefly.

2.1.1 Underbalanced Drilling

During UBD operations, a low density drilling fluid is used in order to maintain a wellbore pressure profile that is lower than the pore pressure of the formation at all locations along the borehole. One major advantage of UBD over conventional drilling is that formation damage is reduced because a filter-cake is not allowed to form near the wellbore. Wells completed with UBD have been shown to perform three to four times better than their conventional counterparts in the same formation (Ramalho 2006). In addition, lost circulation can often occur during conventional drilling when a large fracture is either created or encountered. Massive mud losses into the fracture can cause a complete loss of drilling fluid circulation resulting in extremely long and uneconomic nonproductive times. UBD techniques can often help to avoid these costly lost circulation situations. An additional benefit that cannot be understated is that UBD can greatly enhance the ROP, as illustrated in **Figure 2.1**, especially in tight-hard-rock reservoirs (Ramalho et al. 2009). This phenomenon is not well understood, but it is thought that the increased ROP can be attributed to the lower confining pressure on the formation rock under UBD conditions and the fact that cuttings are more easily flushed from the bottom of the wellbore reducing the resistance on the drill bit.

While UBD offers many advantages when drilling into tight gas formations, perhaps the most useful aspect of the technique comes from the insight that can be gained from a variety of data that can be acquired only while drilling underbalanced. The deliberate underbalanced pressure difference between the drilling fluid and the formation pressure causes an inflow of formation fluid into the wellbore along the entire drilled section. The inflow can be measured or determined through various methods and can be used as an indication of different reservoir properties. When applied appropriately, UBD data can be used to enhance our understanding of several attributes of the target formation that have significant economic implications, including the distribution of fluids within the targeted zones, potential well productivity, and optimal well trajectory and completion strategies (Ramalho et al. 2009).

Procedures that make use of UBD data have been described as dynamic reservoir characterization techniques. **Figure 2.2** is a good illustration of how the technical advantages of UBD translate into economic benefits. It is clear that UBD presents the opportunity for real-time decision making regarding drilling and well completion strategies. Specifically, the knowledge of the location of potentially productive fracture zones can influence where engineers decide to stimulate hydraulic fractures (King 2010). In addition, comparison of the early-time UBD data with more conventional well testing methods can help to improve accuracy of estimates of reservoir properties.

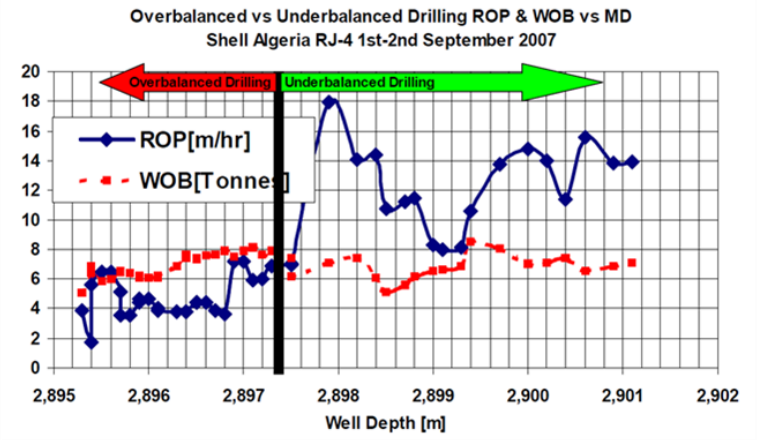

Figure 2.1 Data from a well drilled overbalanced until a certain depth and then switching to underbalanced operations. Immediately as UBD begins, the ROP greatly increases. (Woodrow et al. 2008).

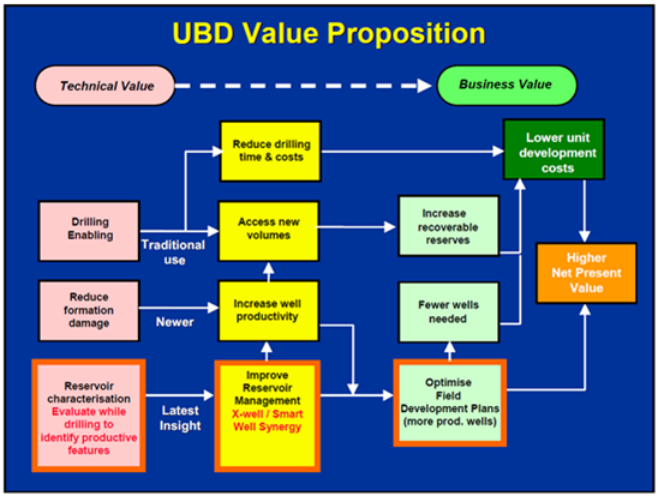

Figure 2.2 This diagram illustrates how the technical advantages of UBD eventually lead to economic value throughout the development and production life of a well. (Woodrow et al., 2008).

2.1.2 Hydraulic Fracturing

The difficulty in producing from unconventional reservoirs stems from the fact that these formations are extremely impermeable or "tight". The inability of fluid to flow through these formations has extreme economic implications. While conventional reservoirs often have recovery rates of more than 80% of OGIP, many unconventional plays have been estimated to recover less than 2% of OGIP without stimulation (King 2010; Moore 2010). In order to be considered economic, unconventional reservoirs must undergo massive hydraulic fracture stimulation. Hydraulic fracturing operations can greatly enhance the effective permeability of the formation by increasing the connectivity of the natural fractures that are present.

Natural fractures within a formation are usually unproductive because they are not connected to each other. Only once they have been opened and connected through hydraulic fracturing do they become productive. However, the locations of these natural fractures are often widely unknown and the process for selecting hydraulic fracture initiation points is somewhat arbitrary. Currently, the most widely used method for selecting hydraulic fracture initiation points is to simply place them at equally spaced segments along the horizontal portion of the well. In practice, this method can often damage the natural fracture system or completely miss the fractured zones.

Hydraulic fracturing techniques have been researched thoroughly for several decades. Techniques have undergone remarkable developments within the last few years that have enabled production from many new tight gas reservoirs. These developments include slickwater fracturing, multi-stage fracturing, and the use of horizontal wells instead of vertical wells. Through these developments, EUR's have increased from roughly 2% to nearly 50% in tight gas reservoirs (King 2010). Even though state of the art in hydraulic fracturing has enabled large scale production from unconventional gas fields, there is still much to be learned in order to maximize production while minimizing risk to the petroleum industry, the public, and the environment.

2.2 Natural Fracture Characterization from Image Log and Core Analysis

Techniques for directly assessing near wellbore fracture density, fracture aperture, and fracture orientation are presently available to the industry by means of image log testing. Examples of image log techniques include borehole video camera, acoustic formation image technology (AFIT), and resistivity image logs. These three methods are based on different fundamental principles, and each has its own set of advantages and disadvantages. A common

drawback is that the image resolution quality is generally too poor to be able to identify conductive features that are believed to be on the order of 100 μm wide. When core samples are available, core analysis can also be a very effective tool for characterizing natural fractures. A description of each characterization method and an overview of the various analyses performed using the respective data is presented in this section.

Perhaps the most intuitive method one can think of to gain information about natural fractures that intersect a wellbore is to employ a camera downhole to make visual observations. Conventionally, borehole video cameras have been used in oil and gas wells to investigate wellbore integrity, but they have also been utilized for the purposes of natural fracture characterization with limited success. One report by Overbey et al. (1988) presents a horizontal well drilled with air in which borehole video was used to identify fractures. The wellbore was clean and free of debris. More than 200 features were identified as natural fractures over the 2,217 feet of wellbore that was surveyed with the video camera. The report presents an approach to interpret the fracture orientation based on the geometry of the observed feature. The report makes no attempt to quantify the aperture of the features identified or to distinguish between conductive and non-conductive features. The report concludes that borehole video cameras can be implemented as a natural fracture identification technique in air-drilled horizontal wells in low-pressured reservoirs.

The use of AFIT has been implemented to characterize the permeability of feed zones in oil and gas and geothermal wells. A description of the AFIT tool is given by McLean and McNamara (2011):

> As the AFIT tool is lowered and raised in the well an acoustic transducer emits a sonic pulse. This pulse is reflected from a rotating, concave mirror in the tool head, focusing the pulse and sending it out into the borehole. The sonic pulse travels through the borehole fluid until it encounters the borehole wall. There the sonic pulse is attenuated and some of the energy of the pulse is reflected back towards the tool. This is reflected off the mirror back to the receiver and the travel time and amplitude of the returning sonic pulse is recorded. Through the use of the rotating mirror (≤ 5 rev/sec) 360° coverage of the inside of the borehole wall can be obtained (McLean and McNamara 2011).

In practice, the interpretation of AFIT data is quite sophisticated. Planar natural fractures appear as sinusoids in the imaged data set (see **Figure 2.3**). Data processing software allows for

characterization of geologic features including strike and dip, fracture aperture, and fracture density. The signal amplitude can be used to distinguish between open and closed fractures. Low amplitude signals are seen as a dark features on the acoustic image and often interpreted as open. High amplitude signals are seen as light features on the acoustic image and are thought to be attributed to mineral fill. These high amplitude features are usually considered closed fractures that do not contribute to flow. While McLean and McNamara (2011) report a good level of correlation between measured feedzone fluid velocity and fracture aperture determined from AFIT, the fracture apertures reported range from several centimeters to greater than 50 cm. This implies that the resolution of AFIT can at best distinguish fractures of roughly one to two centimeters. This is nowhere near the level of resolution quality necessary for fracture characterization in highly fractured tight gas reservoirs.

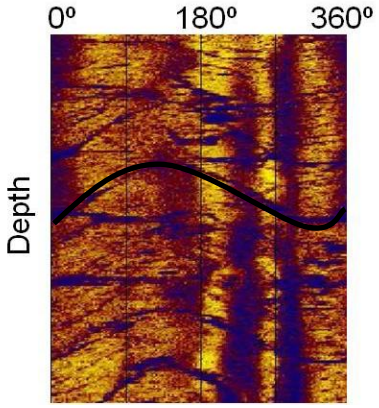

Figure 2.3 Example of an AFIT image log. The vertical axis is depth. The horizontal axis is azimuth around the wellbore. The sinusoids are interpreted as planar geologic features. (Mclean and McNamara 2011).

Resistivity image logs, also called formation micro-image (FMI) logs, have been documented as an improved technique to characterize geologic features along the wellbore. These techniques make use of a tool that places an electrode at constant electrical potential against the borehole wall and measuring the current. One type of microresistivity imaging tool is described by Kalathingal and Kuchinski (2010) (see **Figure 2.4**). The tool is a small-diameter imaging tool that can be deployed with or without a wireline. The high sampling density of these tools (e.g., 120 samples per foot) provides extremely high resolution in the image quality. Microresistivity imaging tools have the ability to visualize features down to 2 mm in width. Careful interpretation of resistivity image logs can provide helpful information about the geologic conditions near wellbore, including dip analysis, structural boundary interpretation, fracture characterization, fracture description, and fracture distribution.

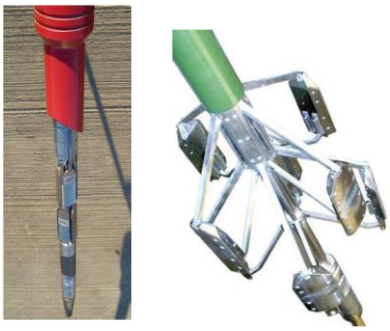

Figure 2.4 Photograph of a microresistivity imaging device (left) passing through drillpipe and (right) in the open position. (Kalathingal and Kuchinski 2010).

Data obtained from all three of these image log techniques can be analyzed to gain useful insight about the natural fracture system and state of stress system near wellbore. Barton and Zoback (2002) present an approach for discriminating natural fractures from drilling induced fractures from different types of image logs, and using this knowledge to determine the state of stress in-situ. It has been well documented that drilling induced tensile fractures will form in the azimuth of the maximum horizontal principal stress. Alternatively, compressive stresses concentrate in the azimuth of minimum horizontal principal stress, and shear failure in this region often causes breakout to occur (see **Figure 2.5**). If the three in-situ principal stresses can be determined and the formation fluid pressure is known, then a Coulomb failure analysis can be applied to the natural fractures identified in the image logs. Shear and effective normal stresses acting on each fracture plane can be determined from knowledge of the orientation of the fracture plane with respect to the orientations of the principal stresses. The Mohr-Coulomb failure envelope for fractures is determined from laboratory measurements on prefractured rock. The failure line is constructed assuming no cohesion and using the friction angle of the prefractured rock. Poles to fracture planes are then displayed on the Mohr diagram. Critically stressed fracture planes lie above the Mohr-Coulomb failure envelope (see **Figure 2.6**). Barton and Zoback (2002) report a strong correlation between critically stressed fracture planes and hydraulic conductivity of the fractures. These findings indicate that only a small percentage of the total number of fractures are likely to contribute to flow.

The most direct method for characterizing the natural fractures present in the reservoir is to perform core sample analyses. Fracture density and fracture spacing can be determined through visual analysis of the core (e.g., Gale et al. 2007; Kubik and Lowry 1993). Plugs are typically taken for laboratory experiments to measure permeability and other flow properties. These experiments can only measure an "effective" permeability of the core sample. Generally, it is not possible to determine the natural fracture contribution to flow unless the fracture geometry

is well known. The key issue, however, is that experience has shown that using laboratory measurements to represent reservoir-scale properties can be vastly misleading. Nonetheless, engineers are faced with the challenge of interpreting the few available direct measurements of the reservoir rock and translating them to field-scale properties.

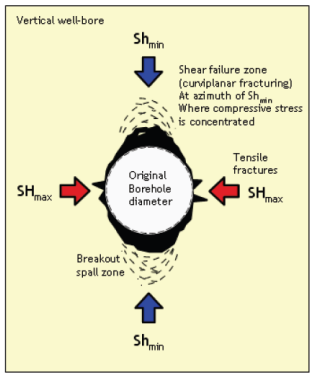

Figure 2.5 Illustration of wellbore stability fundamentals. Drilling induced tensile fractures occur in the direction of the maximum horizontal stress. Compressive stresses concentrate in the direction of minimum horizontal stress, and shear failure in this region can cause breakout to occur. (Kalathingal and Kuchinski 2010).

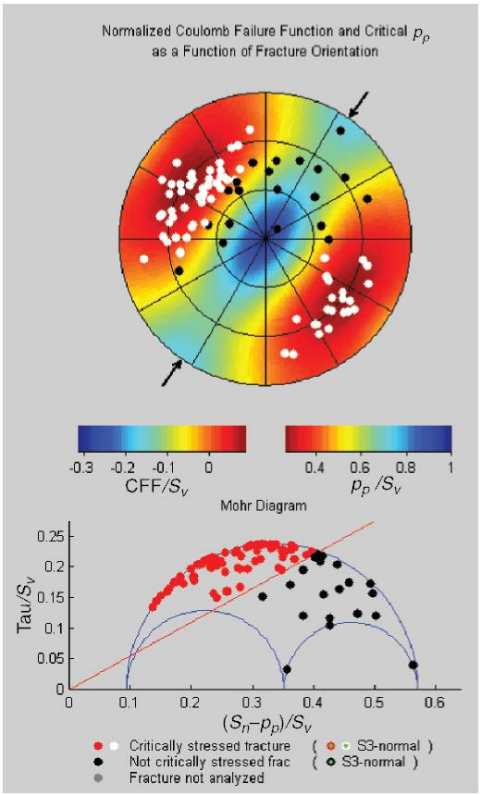

Figure 2.6 These figures illustrate the concept that critically stressed natural fractures predominantly contribute to fluid flow through reservoirs. (Barton and Zoback 2002).

2.3 Natural Fracture Characterization in Real-Time

Recently, there has been much literature generated attempting to characterize fractures and formations using data that is obtained while drilling. Early estimates of reservoir permeability and location of natural fractures have significant economic impacts and can help reservoir and drilling engineers to make real-time decisions during drilling to optimize the completion process. Many analysis methods, such as core description or image log analysis, cannot distinguish conductive natural fractures from those that are practically impermeable because they do not measure fluid flow properties directly (Dyke et al. 1995). While core sample analyses may be able to measure flow rates and permeabilities across the entire sample, it is not possible to directly quantify the flow within the natural fractures.

Fracture characterization during conventional overbalanced drilling has been studied in depth since the 1990's (e.g., Dyke et al. 1995; Sanfillippo et al. 1997; Liétard et al. 1999; Verga et al. 2000; Lavrov and Tronvoll 2003; Majidi et al. 2008a; Majidi et al. 2008b; Huang et al. 2010). These publications use mud-loss data acquired during drilling in order to characterize fracture width. UBD dynamic reservoir characterization has also been employed as a method to quantify formation parameters while drilling (Ramalho 2006; Ramalho et al. 2009). While methods to estimate formation parameters during UBD have been successful, methods to provide real-time estimates of natural fracture characteristics during UBD have received limited discussion.

2.3.1 Overbalanced Drilling Methods

Overbalanced drilling approaches for fracture characterization mostly consist of methods that take advantage of mud-loss data and the rheological properties of the circulating drilling fluid. Drilling mud is usually a non-Newtonian fluid that exhibits shear-thinning behavior. Shear-thinning implies that the fluid viscosity decreases with an increase in the shear rate. During drilling, the drilling mud is constantly circulated through a closed-loop system. If the circulation is stopped, the drilling mud will develop into a thick gel. The mud will remain in this state until a pressure exceeding the mud's yield stress is applied, at which point it will return to its "fluid" state. This non-ideal fluid behavior has allowed engineers to develop methods to characterize fracture permeability using mud-loss data.

During overbalanced drilling, when a sweet spot is encountered the mud pressure is greater than the fluid pressure contained in the fracture resulting in a flood of drilling mud into the fracture (**Figure 2.7**). At the surface, this is observed as a loss of volume in the mud pit

which can be measured. The mud losses eventually stop once the difference between the pressure driving the mud and the fluid pressure in the fracture is equal to the yield stress of the drilling mud. Liétard et al. (1999) provide type curves describing mud loss volume versus time that can be used to determine the hydraulic width of fractures through a curve matching approach. The type curves are based on an analysis of the local pressure drop in the fracture (Liétard et al. 1999):

$$\frac{dP}{dr} = \frac{12\mu_p v_m}{w^2} + \frac{3\tau_y}{w} \tag{2.1}$$

Here v_m is the local velocity of the mud in the fracture, μ_p is the plastic viscosity of the mud, w is the fracture aperture, and τ_y is the yield stress of the mud.

Huang et al. (2010) improved upon the work of Liétard et al. (1999) by deriving a cubic equation in fracture aperture, w, with coefficients dependent on known values of well radius, R_w, overpressure ratio, $\Delta P_{OB}/\tau_y$, and the maximum mud-loss volume, $(V_m)_{\max}$:

$$\left(\frac{\Delta P_{OB}}{\tau_y}\right)^2 w^3 + 6R_w\left(\frac{\Delta P_{OB}}{\tau_y}\right)w^2 - \frac{9}{\pi}(V_m)_{\max} = 0 \tag{2.2}$$

Using root finding techniques, this equation can be solved for the hydraulic width of the fracture. This method is much simpler to use than the curve matching techniques previously employed while providing consistent results.

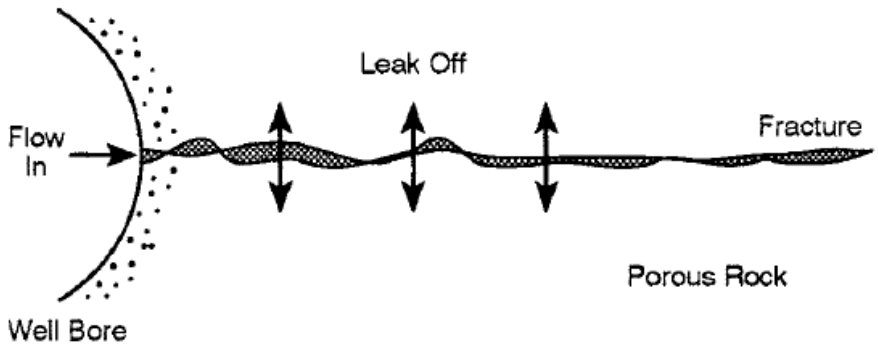

Figure 2.7 During conventional (overbalanced) drilling, the mud pressure in the wellbore is greater than the fluid pressure contained in the fracture. When the drill bit intersects the fracture drilling mud will flow into the fracture. In reality some leak off into the formation will occur, however it is commonly assumed that the formation permeability is sufficiently low to prevent any leak off. (Dyke et al. 1995).

2.3.2 Underbalanced Drilling Methods

As discussed in previous sections, underbalanced drilling provides many benefits to a drill team (increased rate of penetration, decreased formation damage, reduction of lost circulation). Engineers have also realized that since the well is actually producing hydrocarbons during the drilling process, analysis of UBD data can provide information similar to that of a pressure transient test (Kardolus and van Kruijsdijk 1997). The production rates offer an opportunity to evaluate formation properties in real-time. Several methods have been proposed in the literature (e.g., Kardolus and van Kruijsdijk 1997; Larsen and Nilsen 1999; Hunt and Rester 2000; Kneissl 2001; Biswas et al. 2003; Erlend et al. 2003; Friedel et al. 2008).

All methods are based upon data that can be acquired while drilling underbalanced. The most important piece of data is the rate of fluid flow from the formation into the wellbore. Very rarely are flow rates actually measured at bottomhole. In almost all cases, the formation fluid flow rate is estimated from surface measurements of inflow and outflow of the drilling fluid. The difference between the mud injected into the wellbore and the outflow of mud from the annulus is often estimated as the formation fluid flow rate. Methods to account for the expansion of gas due to changes in temperature and pressure must be taken into account to obtain accurate data (Aremu and Osisanya 2008). Other data that models tend to utilize include: bottomhole pressure, rate of penetration, formation porosity, wellbore diameter, and wellbore length. Models generally provide profiles of formation permeability and pore pressure versus depth.

Models are usually derived from the diffusivity equation for single phase, slightly compressible fluid flow through porous media (see Equation 1.13). Applying Equation 1.13 to drilling, however, can be difficult due to the fact that boundary conditions change with time during the drilling process. Specifically, the wellbore length and bottomhole pressures are changing with time. Modeling this behavior has been attempted using the boundary element method (BEM) (e.g., Kardolus and van Kruysdijk 1997). These methods are not necessarily useful for calculator or spreadsheet analysis, and therefore have limited practical value to engineers wishing to make real-time decisions. Additionally, the reports discussed in this section thus far do not address the application of their methodologies to characterization of natural fracture systems.

Some reports in the literature discuss the idea of using UBD data to characterize natural fracture systems, but very few present case studies. At least one report has indicated an attempt to use mud log gas shows as a means to detect natural fracture locations while drilling

underbalanced (Myal and Frohne 1992). The report investigates the effectiveness of directional drilling in a tight gas formation located in the Piceance Basin of Western Colorado. The formation is known to be highly naturally fractured, and consequently the decision was made to drill a large section of the well underbalanced in order to reduce formation damage and lost circulation. From analysis of the mud log it is clear that at least ten major gas shows were detected (see **Figure 2.8**). These gas shows were attributed to the presence of natural fractures intersected by the wellbore. No effort was made to characterize the permeability of each of the natural fractures in this particular study, however, it is conceivable that the persistence of the gas shows could be correlated to productivity or permeability.

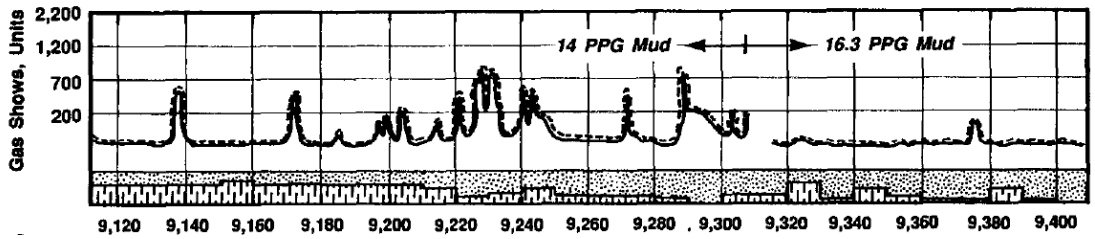

Figure 2.8 Mud log data from a portion of a well drilled underbalanced in the Piceance Basin. The large gas peaks were attributed to natural fractures that were intersected by the wellbore. (Myal and Frohne 1992).

CHAPTER 3: METHODOLOGIES

The purpose of the present study is to determine whether it is feasible to use UBD data to gain useful information about the condition of the natural fracture system near the wellbore. The hypothesis is that if a natural fracture is intersected by the wellbore while an underbalanced pressure condition exists at bottomhole, then a rapid influx of the gas originally contained within the natural fracture will occur into the wellbore. The influx will occur almost instantaneously due to the extremely high permeability of the fracture. The possibility exists that several indicators of this phenomenon can be observed in the drilling log and mud log data. Since this data is recorded for virtually every new well that is drilled, it is extremely practical to investigate the ability to gain useful information about the natural fracture system from these logs.

The methodologies described in this section have two primary stages. The first stage is to determine the locations along the wellbore where natural fractures are highly likely to be present. In order to accomplish this task, two types of data from drilling and mud logs are used as indicators of the presence of natural fractures. These indicators are total gas concentration and mud pit volume response. If these two indicators occur simultaneously at a particular location along the wellbore, then this location is considered a "candidate conductive natural fracture location." Once all of the candidate natural fracture locations have been identified, then the next task is to characterize the permeability of each of the fractures. The width of the natural fracture can be determined through use of the cubic law and estimates of gas flow rate through the fracture. The flow rate of gas is estimated from the mud pit volume response.

3.1 Natural Fracture Location

Methods to determine the location of natural fractures that intersect wellbores through the use of UBD data have been developed. There are two types of data found in the drilling log and mud log that have been explored as criteria for indicating the location of natural fractures along the wellbore. The basis for the use of these data for natural fracture identification is founded on physical processes as well as drilling engineering experience.

The first criterion is the use of total gas concentration measurements from mud logs. Using a gas chromatograph, the mud logging unit is able to determine the concentration of gas present in the drilling fluid at any given time. The hypothesis is that as a natural fracture is encountered by the drill bit, the volume of gas contained within the fracture will rapidly flow into the wellbore and enter the stream of circulating drilling fluid. This will be seen as a sudden "spike" in total gas concentration in the mud log, which will eventually return to normal

operating levels after all of the trapped gas has exited the fracture (see **Figure 3.1**). For the purposes of the present research, these spikes have been expressed as "gas peaks", and offer the potential for reliably locating conductive natural features.

The second criterion is based on observations of the mud pit volume. Observations of the mud pit volume at the surface also show potential as a fracture identification criterion. It is widely accepted that decreases in mud pit volume (mud losses) correspond to encounters with natural fractures while drilling overbalanced. Drilling engineers have indicated that they are confident that the "reverse" case is also true during underbalanced drilling operations. While underbalanced conditions exist in the wellbore, as a natural fracture is encountered with the drill bit, the formation fluid influx will cause a displacement of drilling fluid in the mud pit. This response is observable at the surface. An increase in the mud pit volume has been termed a "mud pit volume peak" for the purposes of this research. Determining the location of the drill bit as relatively large mud pit volume increases are observed at the surface will be used as an indicator of natural fractures.

Members from industry are confident that the gas peak (Criterion 1) and mud pit volume peak (Criterion 2) criteria are good indicators of conductive natural fractures. Thus, Criteria 1 and 2 are used to identify candidate natural fracture locations.

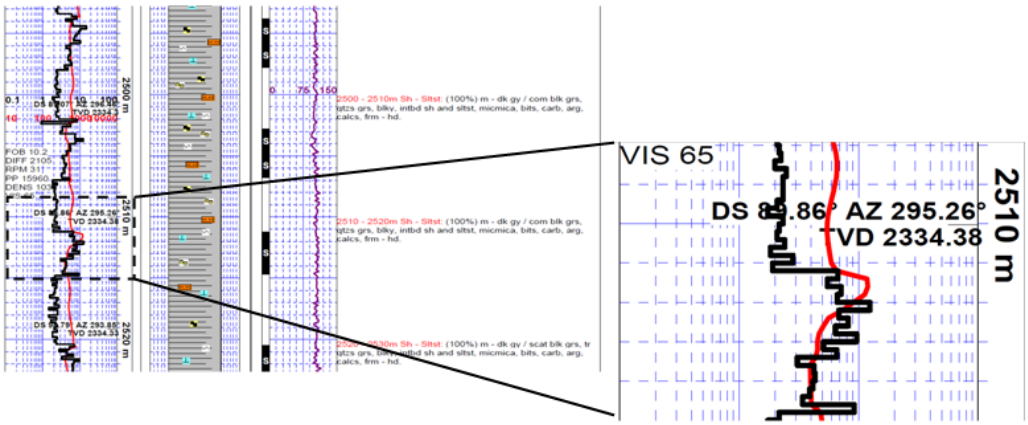

Figure 3.1 Example of a mud log. (Left) A mud log contains many types of information recorded during drilling operations including ROP, gamma ray, total gas, and lithology. (Right) The red line represents total gas. Total gas spikes are used to identify productive features (natural fractures) during drilling.

3.2 Natural Fracture Permeability

The major advantage of using underbalanced drilling data over image log techniques is that UBD data provides the opportunity to distinguish natural fractures that actually contribute to

flow from fractures that are essentially closed. Since the rates of gas influx from the natural fractures are being measured directly, the fluid flow properties of the fractures, most notably permeability, can be estimated. This concept is truly what makes the prospect of UBD dynamic reservoir characterization so exciting.

In order to estimate natural fracture permeability, several assumptions are made:

1. All natural fractures that have been intersected by the wellbore are transverse to the wellbore and have circular geometry with finite extent (see **Figure 3.2**).
2. Natural fractures have constant aperture.
3. Gas contained within natural fractures is composed 100% of methane. Methane density and viscosity remain constant while flowing through fractures.
4. Fluid flow through fractures follows the cubic law relationship.
5. Matrix permeability is much lower than fracture permeability. No charging of the fractures occurs during the time spans considered.
6. The gas influx volume is equal to the mud pit volume increase.

For practical purposes, the first three assumptions are valid. Some work has been done on the effects of tortuosity and roughness of fractures, and this could be included in the model if enough information is known. The radial extent of the natural fracture must be estimated by the user. A sensitivity study could be performed to quantify the effect of fracture diameter on the estimates of fracture aperture.

The cubic law relationship assumes steady-state, laminar flow between two parallel plates. The cubic law can be derived from a force balance between the forces due to the pressure gradient and the shear resistance on the boundaries, as opposed to the diffusivity equation which is derived using the principles of conservation of mass. As such, no compressibility term is present in the cubic law relationship. However, the high compressibility of gas will most likely have significant effects on the flow rate through the fracture. Nonetheless, it is assumed that at the high pressure conditions present in the reservoir, compressibility effects will be negligible over the relatively low magnitude pressure drop between reservoir and bottomhole pressures.

The final assumption is the most critical. Because no direct measurements of gas flow rate at bottomhole are recorded on today's drilling rigs, it is assumed that the observed mud pit volume increase is equal to the volume of gas that entered the wellbore from the fracture. Again, compressibility effects could be significant and add to the uncertainty of this analysis. Also, it is

well known that methane is highly soluble in oil-based drilling mud, and it is has been reported that observations of mud pit volume increase as a response to a gas kick will be reduced because of solubility effects.

The following estimates can be obtained from the drilling and mud log data:

- Gas flow rate
- Pressure drop (underbalance)
- Methane viscosity
- Wellbore radius

If an assumption about the radial extent of the fracture can be made, then fracture aperture can be determined as follows:

$$w = \left(\frac{Q}{C\Delta P} \right)^{1/3} \tag{3.1}$$

The fracture permeability can then be estimated using Equation 1.17.

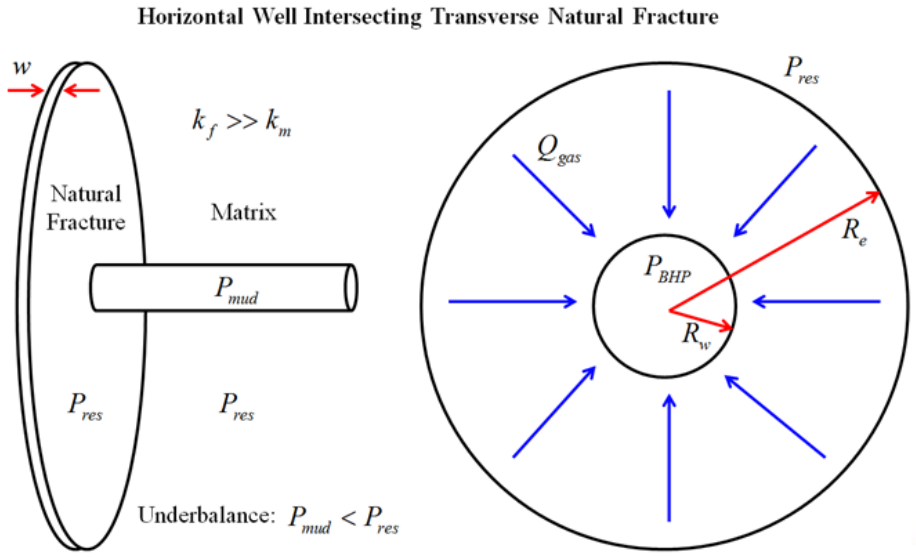

Figure 3.2 Illustration of the model used for characterization of natural fracture permeability. It is possible to estimate natural fracture permeability using measurements of gas influx rate recorded during drilling.

CHAPTER 4: DEVELOPMENT OF COMPUTATIONAL TOOL

The drilling and mud log data are typically presented in Excel spreadsheet format. The data are recorded on a depth basis at constant intervals (e.g., every 0.5 feet). The length of the horizontal segment of wellbores drilled in tight gas reservoirs usually ranges from 4,000 to 6,000 ft. The data sets prepared for this study are extremely large, and the length of the data arrays is inconsistent between wells. Processing this amount of data by hand is clearly impractical, and the use of a spreadsheet analysis is very cumbersome. Hence, a computational tool has been developed using the MATLAB framework.

The tool is capable of determining the locations of conductive natural fracture zones, subject to a set of fracture identification criteria. Once the candidate natural fracture locations have been determined, the tool then calculates the fracture permeability at each of these locations. Engineers must be able to apply the computational tool with relative ease and little training. MATLAB was chosen as the appropriate software for this analysis because it has the ability to interact with Excel. Input data is prepared in an Excel spreadsheet template, the analysis is performed through MATLAB, and the output data is exported back into an Excel spreadsheet. Several useful charts are also exported within the MATLAB framework.

The program developed in this research for characterizing the natural fracture system near the wellbore in wells drilled underbalanced is called `fracid_ubd`.

4.1 Input Data and Data Preparation

Most drilling logs and mud logs come in the form of Excel spreadsheets or can be transformed into Excel spreadsheets. In accordance with this convention, an Excel spreadsheet template has been created to prepare the input data for `fracid_ubd` (see **Figure 4.1**). There are six arrays of data from the drilling and mud logs to be stored: measured depth, true vertical depth, rate of penetration, drilling mud density, mud pit volume, and total gas concentration. Only the data corresponding to the horizontal section of the wellbore is relevant to this analysis; all data corresponding to the vertical and heel sections of the well must be removed. Special care must be taken to remove any "connection gas" events due to drillstring connections from the total gas array (see **Section 1.2**). This step is imperative to the analysis, as the connection gas events will appear as large gas peaks and could be mistaken for the presence of natural fractures. These mechanically induced gas peaks will also negatively impact the fracture identification procedure. In many instances, the drillstring connections will cause disruptions in the mud pit volume measurements and should be accounted for.

Three additional input values are required for the analysis: ratio of radial extent of fracture to wellbore radius, average reservoir pressure, and unit type. In order to characterize the permeability of the candidate natural fractures, an assumption must be made about the radial extent of the fracture. This parameter can be chosen and adjusted by the user to investigate the effect of fracture diameter on the estimate of fracture permeability. In order to estimate the level of underbalance, the reservoir pressure in-situ must be known. In practice, the reservoir pressure is not well known at all locations along the wellbore. An estimate of the reservoir pressure for a given well can often be determined from well tests or empirical relationships. Finally, `fracid_ubd` has been designed to operate in both metric units and U.S. oil field units. A binary system is used to indicate the appropriate unit system for the analysis according to the log data. The user must enter 0 or 1 to specify metric units or U.S. oil field units, respectively.

Drilling Data						Misc. Input Data		
Measured Depth (m) (ft)	True Vertical Depth (m) (ft)	Rate of Penetration (m/s) (ft/hr)	Mud Density (kg/m^3) (lb/gal)	Mud Pit Volume (m^3) (bbls)	Total Gas (units) (units)	Ratio of Radial Extent of Fracture to Well Radius (R_e/R_w)	Average Reservoir Pressure (kPa) (psi)	Unit Type 0 = Metric 1 = U.S. Oil Field
12840.0	12412.1	30.5	16.0	601.2	783	50	11575	1
12841.0	12412.1	35.2	16.0	601.7	759			
12842.0	12412.1	32.8	16.0	601.7	737			
12843.0	12412.1	33.9	16.0	602.2	697			
12844.0	12412.2	33.9	16.0	602.2	785			
12845.0	12412.2	33.4	16.0	602.7	706			
12846.0	12412.2	33.8	16.0	602.6	733			
12847.0	12412.2	30.3	16.0	603.0	739			
12848.0	12412.3	33.9	16.0	603.1	783			
12849.0	12412.3	32.1	16.0	603.0	828			
12850.0	12412.3	34.5	16.0	603.1	787			
12851.0	12412.3	31.6	16.0	603.3	749			
12852.0	12412.3	33.8	16.0	603.0	649			

Figure 4.1 Example of the Excel spreadsheet template used to prepare the input data for the computational tool; spreadsheet is populated with example input data.

4.2 Computational Procedure

In the following sections the computational routine is deconstructed into three stages: preliminary operations, determination of the locations of conductive natural fracture zones, and characterization of fracture permeability at these locations. The steps taken to process the drilling and mud log data are described briefly. For a more detailed description of the code see the user's manual (see **Appendix A**).

4.2.1 Preliminary Operations

The input data file is read through a MATLAB command called `xlsread`. This command provides the link between Excel and MATLAB frameworks. In many instances, the drilling and mud log data contain several missing or erroneous values due to equipment errors, so once the data has been stored a simple routine is performed to resolve any erroneous points within

the data. This is done by replacing the erroneous value with the value of the previous step. It should be noted that there must be no missing or erroneous values contained in the measured depth data array.

The ROP data array is used to create a time series consisting of elapsed time between intervals. This will later be used to estimate gas influx rates. The downhole pressure is calculated using the mud density and true vertical depth measurements:

$$P_{DHP} = \gamma_{mud} D_{TVD} + \Delta P_{ann} \tag{4.1}$$

Here P_{DHP} is the downhole pressure, γ_{mud} is the mud density gradient or unit weight of the drilling mud, D_{TVD} is the true vertical depth, and ΔP_{ann} represents the frictional losses through the annulus. The pressure loss term is positive because the direction of the flow in the annulus is upwards, and the frictional force acts in the opposite direction to flow. In this analysis, the frictional losses through the annulus are assumed to be zero. This will be shown to be a conservative assumption.

4.2.2 Natural Fracture Locations

As discussed in **Section 3.1**, conductive natural fracture locations are determined using a set of fracture identification criteria. It is reasonable to assume that a fracture may exist at locations where all fracture identification criteria are satisfied simultaneously. Additionally, a threshold must be established to determine the magnitude of total gas and mud pit volume response that will be considered as an indication of the presence of a natural fracture. The concept of the "standard deviation coefficient" is now introduced.

In order to ensure the portability of the code between data sets collected at different wells or by different contracting companies, a general statistical approach is used to process the total gas and mud pit volume data. The premise for this analysis is that any gas peaks or mud pit volume peaks that exceed the average level of noise in the data by some threshold are considered of interest. The following formula is used as a cutoff criterion for a particular measurement:

$$M \geq \mu_M + (N \cdot \sigma_M), \quad N \geq 0 \tag{4.2}$$

Here M is the value of the measurement of interest, μ_M is the mean of all the measurements, σ_M is the standard deviation of all the measurements, and N is the "standard deviation coefficient." The measurements of interest are the changes in total gas concentration and mud pit

volume between two consecutive recordings. The value of N can be controlled by the user to raise the threshold to the desired magnitude. Through the use of Equation 4.2, the user is able to define an appropriate level of stringency on the fracture identification criteria based upon the confidence level in the data.

The mean of all the measurements, μ_M, and standard deviation of all the measurements, σ_M, is computed through the following procedure:

$$M_i = X_i - X_{i-1} \tag{4.3}$$

$$\mu_M = \frac{1}{n-1}\sum_{i=2}^{n}|M_i| \tag{4.4}$$

$$\sigma_M = \sqrt{\frac{1}{n-1}\sum_{i=2}^{n}\left(M_i - \mu_M\right)^2} \tag{4.5}$$

where X is either the total gas concentration or the mud pit volume depending on the criterion of interest, and n is the total number of data entries. Equation 4.3 indicates that the changes in the total gas concentration and mud pit volume measurements are relevant to the present study. This ensures that any sudden spikes in total gas concentration or mud pit volume will be highlighted in the analysis. Using the changes in measurements also has a practical purpose; the method accounts for any gas production from the matrix. While the final step in the analysis will only identify increases in total gas concentration or mud pit volume, a sense of the average level of random noise in the data is quantified in Equation 4.4 through the use of the absolute value function. Equation 4.5 will also provide a sense of the variation within the data.

For a normally distributed random variable, the probabilities that the value of the random variable lies within the range of $\mu_M \pm (N \cdot \sigma_M)$ are well understood. The present analysis takes advantage of this knowledge to define appropriate thresholds for the fracture identification criteria. If a particular measurement has a relatively low probability of occurring with regards to the normal noise found within the data, then perhaps this measurement is the result of abnormal reservoir conditions. If more than one independent, low-probability measurement is observed, then the confidence level in the presence of an abnormal reservoir condition becomes even higher. One abnormal reservoir condition that could be attributed to simultaneous gas peaks and mud pit volume peaks has been previously identified as a conductive natural fracture feature (see **Section**

3.1). Of course, it should be noted that a low-probability event could occur as a result of experimental error as well.

One additional fracture identification criterion is defined to overcome the high variability of the total gas concentration measurements:

$$G_i \geq \frac{1}{50} \sum_{j=i-25}^{i+25} G_j \tag{4.6}$$

where G is total gas concentration. Equation 4.6 effectively represents a rolling average of total gas concentration. This constraint ensures that only true gas peaks will be considered, filtering out any total gas increases that have simply returned to normal operating levels after a short period of low readings.

Three conductive natural fracture criteria have now been established. Equation 4.2 constitutes Criterion 1 and Criterion 2 when applied to total gas concentration and mud pit volume, respectively. Criterion 3 is given by Equation 4.6. The computational tool runs the analysis eleven separate times for values of N ranging from 0 to 1. After all data points have been constrained by these three criteria, the result is a set of highly plausible conductive natural fracture zones for each value of N. These locations are recorded as measured depths along the well. The user is then free to select the most appropriate value of N for a given data set.

4.2.3 Natural Fracture Permeability

At this point in the computational procedure, the candidate locations of conductive natural fracture zones have been established. The goal is to now characterize the permeability of these natural fracture features. This is accomplished through the application of the cubic law relationship for flow through fractures. The model used in this study assumes a circular, transverse fracture with pure methane as the reservoir fluid.

The cubic law is given by Equation 3.1 in terms of fracture aperture. For radial flow, the constant, C, is calculated using Equation 1.16. The user selects a value for the ratio of the radial extent of the fracture to wellbore radius. Estimates for methane viscosity can be determined from tables if the reservoir's temperature and pressure are known or have been estimated (e.g., Gonzalez et al. 1967). Perhaps the least understood term in Equation 3.1 is the gas flow rate from the fracture into the wellbore. Direct measurements of the formation fluid influx rate during UBD are not typically recorded on today's drilling rigs for natural gas wells. Honoring the

requirement that this project must maintain its practicality in industry, the gas influx rate is computed using data that is commonly recorded during UBD operations. **Section 3.2** describes the rationale behind using mud pit volume peaks as a measure of the fluid influx volume. The volume is then transformed into a rate through knowledge of the ROP:

$$\Delta t = \frac{D_{MD,2} - D_{MD,1}}{R} \tag{4.7}$$

$$Q_{gas} = \frac{V_{pit,2} - V_{pit,1}}{\Delta t} \tag{4.8}$$

Here Δt is the elapsed time between measurement intervals, D_{MD} is measured depth, R is rate of penetration, Q_{gas} is the gas influx rate, and V_{pit} is mud pit volume. The remaining term in Equation 3.1 is the pressure loss term. This term effectively represents the pressure difference between the reservoir and the bottomhole pressure in the wellbore during drilling, or level of underbalance:

$$\Delta P_{UB} = P_{res} - P_{BHP} \tag{4.9}$$

Here ΔP_{UB} is the level of underbalance, P_{res} is the reservoir pressure, and P_{BHP} is the bottomhole pressure during drilling. All of the terms on the right hand side of Equation 3.1 have now been determined, and the natural fracture aperture can be calculated. The fracture aperture can then be substituted into Equation 1.17 in order to estimate the permeability of the natural fracture of interest. Note that in Equation 4.1, if annular friction losses were accounted for in the bottomhole pressure calculation, the underbalance would decrease. For the same flow rate in Equation 3.1, fracture aperture increases as underbalance decreases. From this quick analysis, it is clear that the assumption of no annular friction losses leads to a conservative estimate of fracture aperture.

4.3 Output Data

Several pieces of output information are generated for each value of N. First, relevant data is exported to the results section of the Excel spreadsheet template (see **Figure 4.2**). Relevant data includes measured depth locations of conductive natural fractures, fracture aperture, fracture permeability, associated mud pit volume and gas peaks, and level of underbalance at the given fracture location. In addition, the correlation coefficient between mud pit volume peak and gas peak is calculated. This value represents the degree of linear dependence between two

variables. Two helpful plots are also generated. The first illustrates the locations of the natural fractures along the lateral section of the wellbore. The second is a cross-plot of mud pit volume peaks and gas peaks corresponding to each natural fracture location.

Candidate Fracture Locations and Permeabilities						
Candidate Fracture Location (m) (ft)	Fracture Aperture (μm) (μm)	Fracture Permeability (md) (md)	Mud Pit Volume Peak (m^3) (bbls)	Gas Peak (units) (units)	Underbalance (kPa) (psi)	Correlation Coefficient (Mud Pit Volume Peak vs. Gas Peak)
12533.0	115	1.108E+06	4.000	988	1093	0.50
12606.0	252	5.274E+06	50.100	740	1087	
12612.0	129	1.379E+06	7.500	486	1087	
12613.0	111	1.033E+06	6.400	118	1086	
12826.0	137	1.569E+06	3.000	171	1081	
12835.0	206	3.547E+06	3.200	156	1081	
13258.0	189	2.978E+06	3.900	182	1143	
13931.0	284	6.701E+06	6.400	198	1134	
13960.0	165	2.274E+06	2.300	150	1133	
14304.0	104	9.040E+05	2.100	164	1192	
15613.0	138	1.590E+06	1.900	103	1178	

Figure 4.2 Example of the types of output data that are exported into an Excel spreadsheet after the natural fracture identification and characterization analysis has been performed.

CHAPTER 5: APPLICATION OF COMPUTATIONAL TOOL AND VALIDATION

The purpose of this investigation is to evaluate the potential for using drilling data as a practical means for determining natural fracture properties near wellbore. To this end, the methodologies developed in **Chapters 3 and 4** are applied to six wells that were drilled underbalanced. Candidate conductive natural fracture zones are determined for each well. Hence, the natural fracture permeability of each of these zones is estimated.

The wells are from two tight gas shale formations, one located in the U.S. and the other in Canada. The lateral sections of these horizontal wells range from 3,000 to 6,000 ft. It is assumed that no overpressured zones were intersected and the underbalance condition was maintained at all times while drilling the lateral sections of the wells. The lateral sections of all wells were drilled using oil-based mud.

The nature of this problem suggests that it may be very difficult to confirm the accuracy of the results obtained from the fracture characterization analysis. Borehole image logs are not available for any of the wells used for this study, typical of wells drilled in unconventional reservoirs. Therefore, it is necessary to develop validation techniques in an attempt to quantify the level of confidence in the candidate natural fracture locations. The main validation technique used in this study takes advantage of a commonly used horizontal drilling technique in which wells are drilled in parallel. In fact, the six wells selected for study in this investigation constitute three sets of parallel wells drilled to similar elevations. The spacing of these wells is between 500 and 800 ft. The parallel well sets should penetrate similar natural fracture systems. The results of the natural fracture identification analysis for each parallel well set are compared to determine if any patterns exist that may be indicative of the orientation of natural fracture planes.

5.1 Natural Fracture Identification and Characterization Analysis

This project has been highly motivated by concerns from industry that current methods to characterize natural fracture systems are too expensive and often impractical. The computational tool discussed in **Chapter 4** has been designed with ease of implementation as a topmost priority. The analysis makes use only of data that are commonly recorded during underbalanced drilling operations. In this section, field data from wells drilled underbalanced in tight gas reservoirs is processed using the computational tool.

Conductive natural fracture locations are determined according to the fracture identification criteria outlined in **Chapters 3 and 4**. The result is a set of probable conductive

natural fracture zones along the lateral of the wellbore recorded as measured depths. For each conductive natural fracture location, fracture permeability is estimated based on the approach described in **Section 4.2.3**. This estimate for permeability is dependent upon level of underbalance, rise in mud pit volume, and estimate of fracture extent. A chart illustrating the locations of the natural fracture zones along the wellbore accompanied by a table of the estimates of permeability values gives the engineer the ability to effectively visualize the natural fracture system in the near wellbore region. A cross-plot of the mud pit volume peak and gas peak associated with each natural fracture encounter is also provided. It is hypothesized that the magnitudes of the peaks should have a positive correlation based on the underlying physical principles.

Data preparation for this analysis is relatively straightforward. The engineer requires the drilling data log, mud log, and an estimate of average reservoir pore pressure. Data corresponding to the vertical and heel sections of the well are removed. The engineer must then manually remove any noticeable erroneous data points that may be mechanically induced by routine drilling operations. At this point the data is transferred to the provided Excel spreadsheet data input template. The analysis itself runs within seconds. Careful engineering judgment must be used to screen any "false" indicators due to mechanical disruptions to mud pit volume and total gas measurements or data manipulation that were not identified in the data preparation stage. If all of the data sets are available beforehand, it should take the engineer less than one day to prepare the input data, perform the analysis, and analyze the results.

5.1.1 Field A

Two wells have been selected for study from Field A: Well A-1 and Well A-2. The horizontal spacing between these two wells is roughly 800 ft. Well A-1 runs in a South-North orientation and Well A-2 runs in the opposite direction. Well A-1 was drilled toe-down and Well A-2 was drilled toe-up. The geometric properties and the average reservoir pressure for each well, obtained from DFIT testing, are listed in **Table 5.1**. Mud logs are available in *.pdf format for both wells, aiding in the normalization of the total gas and mud pit volume data. The targeted pay zone is roughly 175 feet thick.

Table 5.1 Length of lateral sections, average true vertical depth of lateral sections, and average reservoir pore pressures for corresponding true vertical depth for Wells A-1 and A-2.

Well Name	Length of Lateral (ft)	Average TVD of Lateral (ft)	Average Reservoir Pressure (psi)
A-1	4280.0	12381.8	11550
A-2	3131.0	12389.8	11575

The analysis of Well A-1 indicates that ten conductive natural fractures were intersected during the drilling process (see **Table 5.2**). Two of these natural fractures are within very close proximity to each other and are considered a single conductive natural fracture zone. In total, nine natural fracture zones are present along the lateral of this well. It is clear from **Figure 5.1** that the stretch of lateral between 14,000 and 15,500 ft MD contains no conductive natural fracture zones. This is a primary example of the insight that can be gained from this type of analysis. Decisions regarding hydraulic fracture treatment design can be influenced greatly from knowledge of the extent, or lack thereof, of the natural fracture system. The fracture apertures range from 13 to 53 μm. The cross-plot indicates a general positive correlation between mud pit volume peak and gas peak for these conductive natural fracture zones (see **Figure 5.2**).

Table 5.2 Results from the natural fracture identification analysis for Well A-1.

Well A-1					
Candidate Fracture Location (ft)	Fracture Aperture (μm)	Fracture Permeability (md)	Mud Pit Volume Peak (bbls)	Gas Peak (units)	Underbalance (psi)
12533.0	30	7.500E+04	4.000	988	1093
12826.0	35	1.021E+05	3.000	171	1081
12835.0	53	2.341E+05	3.200	156	1081
12950.0	44	1.613E+05	1.600	286	1080
13235.0	42	1.470E+05	1.700	182	1143
13529.0	37	1.141E+05	1.700	69	1138
13884.0	36	1.080E+05	1.600	74	1135
13960.0	42	1.470E+05	2.300	150	1133
15613.0	35	1.021E+05	1.900	103	1178
16156.0	13	1.408E+04	1.600	644	1234

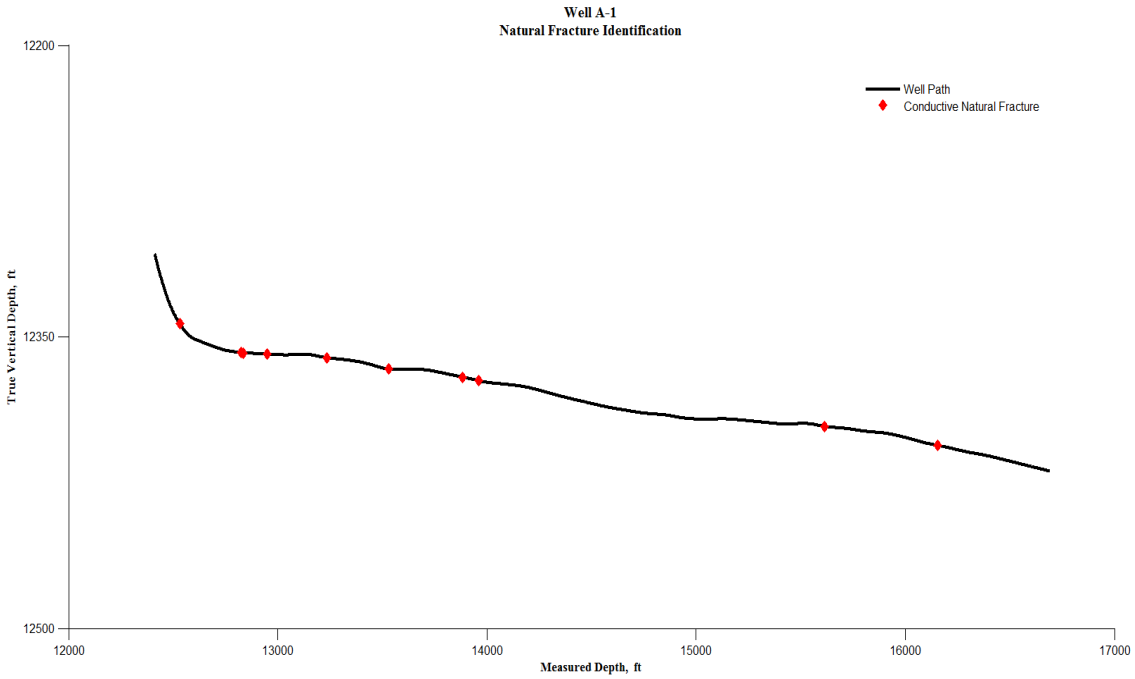

Figure 5.1 Locations of conductive natural fractures along the lateral of Well A-1.

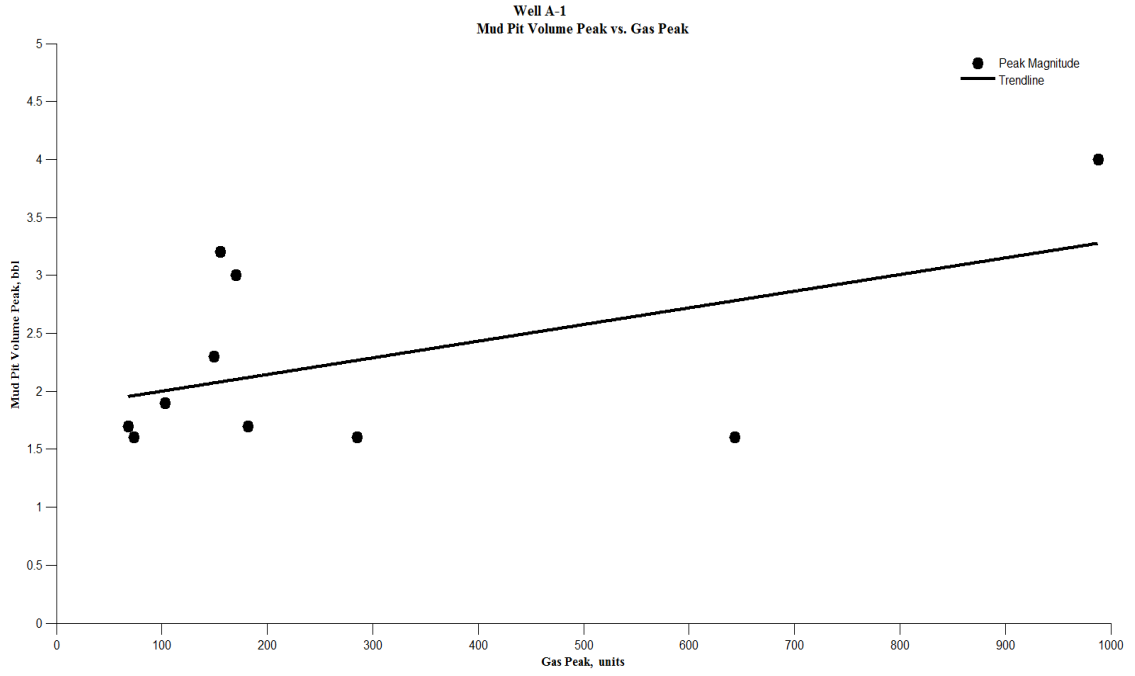

Figure 5.2 Cross-plot of mud pit volume peak vs. gas peak corresponding to each conductive natural fracture location identified for Well A-1.

A total of nine conductive natural fracture zones are identified for Well A-2 (see **Table 5.3**). The zones are relatively evenly spaced along the lateral (see **Figure 5.3**). The fracture apertures are generally smaller than for Well A-1, ranging from 15 to 38 μm. These estimates

could be largely due to the higher level of underbalance maintained while drilling A-2. Additionally, the observed rise in mud pit volume due to the presence of these fractures is relatively low. The cross-plot does not show a strong trend for the relationship between mud pit volume peak and gas peak for these fractures, however, it is a positive correlation (see **Figure 5.4**).

Table 5.3 Results from the natural fracture identification analysis for Well A-2.

Well A-2					
Candidate Fracture Location (ft)	**Fracture Aperture (µm)**	**Fracture Permeability (md)**	**Mud Pit Volume Peak (bbls)**	**Gas Peak (units)**	**Underbalance (psi)**
13467.0	27	6.075E+04	1.177	88	1262
13867.0	29	7.008E+04	0.811	53	1334
13943.0	32	8.533E+04	1.000	75	1335
14192.0	38	1.203E+05	1.176	67	1339
14598.0	16	2.133E+04	0.774	682	1339
14788.0	15	1.875E+04	0.790	328	1336
14990.0	32	8.533E+04	1.170	924	1334
14991.0	35	1.021E+05	1.460	715	1334
15296.0	25	5.208E+04	0.768	70	1338
15750.0	25	5.208E+04	0.930	88	1421

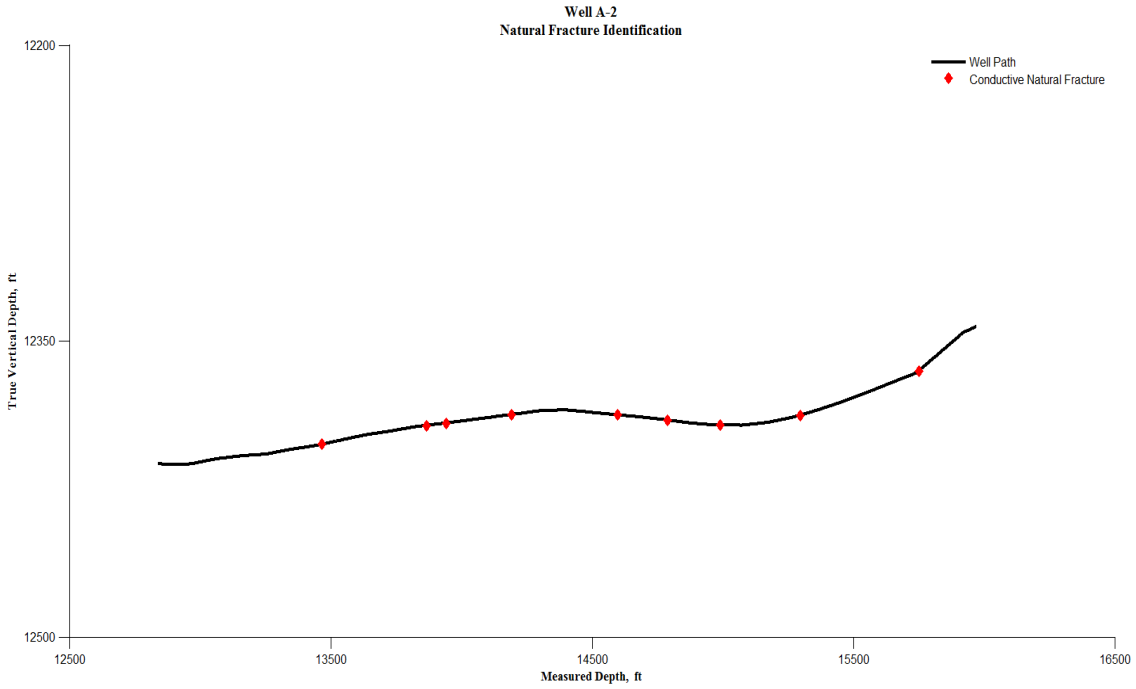

Figure 5.3 Locations of conductive natural fractures along the lateral of Well A-2.

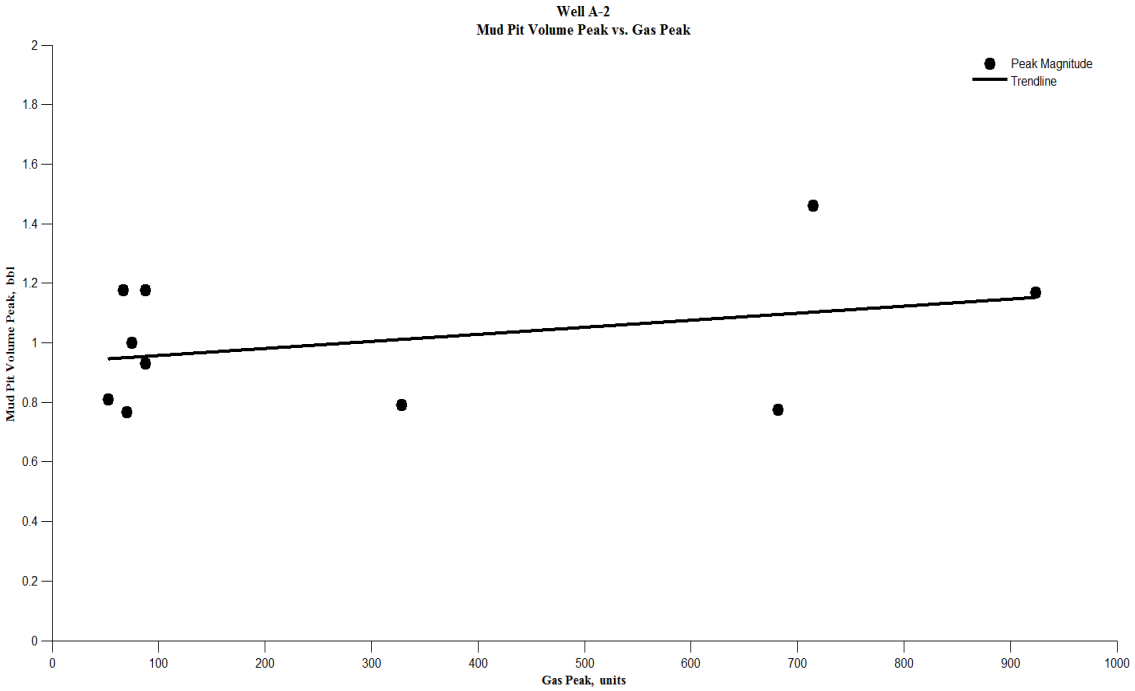

Figure 5.4 Cross-plot of mud pit volume peak vs. gas peak corresponding to each conductive natural fracture location identified for Well A-2.

5.1.2 Field B

Four wells have been selected for study from Field B. These four wells are single lateral wells that were drilled from a common pad. This drilling approach helps to reduce environmental impact and operational costs. These wells were all drilled toe-up. DFIT testing data was not provided for these wells specifically, so reservoir pore pressure was estimated using DFIT data from nearby fields. The average true vertical depth of these wells, and correspondingly the reservoir pore pressure, is quite a bit lower than in Field A. Well geometries and reservoir pore pressure estimates are given in **Table 5.4**. The mud logs for these wells were not provided in *.pdf form, so the exact locations of the drillstring connections are unknown. Care was taken to manually remove obvious connection gas events from the mud log data.

Table 5.4 Length of lateral sections, average true vertical depth of lateral sections, and estimated reservoir pore pressures for the wells in Field B.

Well Name	Length of Lateral (ft)	Average TVD of Lateral (ft)	Average Reservoir Pressure (psi)
B-1	5214.6	8763.5	4641
B-2	4054.5	8726.2	4641
B-3	5676.5	8737.0	4641
B-4	5280.2	8741.8	4641

Out of the total number of natural fractures detected, thirteen conductive natural fracture zones are identified for Well B-1 (see **Table 5.5 and Figure 5.5**). The majority of these zones are located along the first half of the lateral section; only three zones are identified between 12,500 ft and total depth. The estimated fracture apertures are considerably higher than observed in Field A, ranging from 53 to 112 μm. The data in the cross-plot again show a weak positive correlation (see **Figure 5.6**).

Table 5.5 Results from the natural fracture identification analysis for Well B-1.

Well B - 1					
Conductive Natural Fracture Location (ft)	**Aperture (μm)**	**Permeability (md)**	**Mud Pit Volume Peak (bbl)**	**Gas Peak (units)**	**Underbalance (psi)**
10295.2	66	3.63E+05	2.1	96	719
10385.0	69	3.97E+05	1.3	56	719
10498.6	99	8.17E+05	3.2	314	717
10513.7	66	3.63E+05	1.5	143	717
10656.7	99	8.17E+05	4.0	79	720
10832.5	101	8.50E+05	2.9	234	719
10844.4	69	3.97E+05	0.8	33	719
11347.6	76	4.81E+05	0.9	25	720
11560.2	86	6.16E+05	1.0	24	720
11591.1	71	4.20E+05	2.4	24	719
11822.0	112	1.05E+06	3.0	36	718
11887.0	87	6.31E+05	3.0	350	719
11910.6	107	9.54E+05	2.2	62	719
12253.1	88	6.45E+05	2.9	97	725
12289.2	94	7.36E+05	1.5	46	725
13056.3	53	2.34E+05	2.4	519	727
13884.3	53	2.34E+05	1.9	814	734
14113.3	73	4.44E+05	1.8	235	733

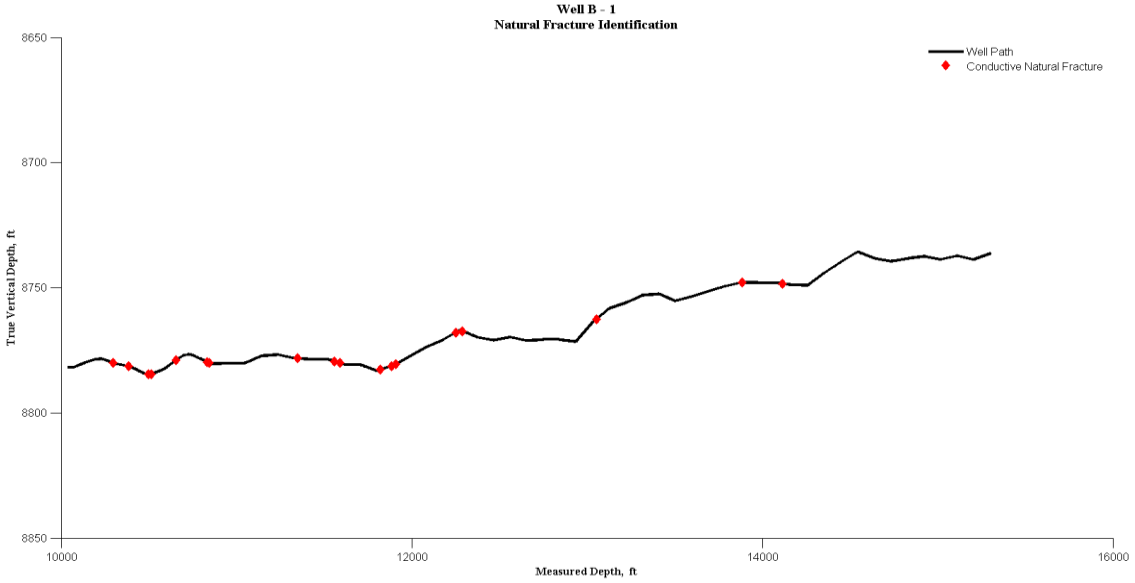

Figure 5.5 Locations of conductive natural fractures along the lateral of Well B-1.

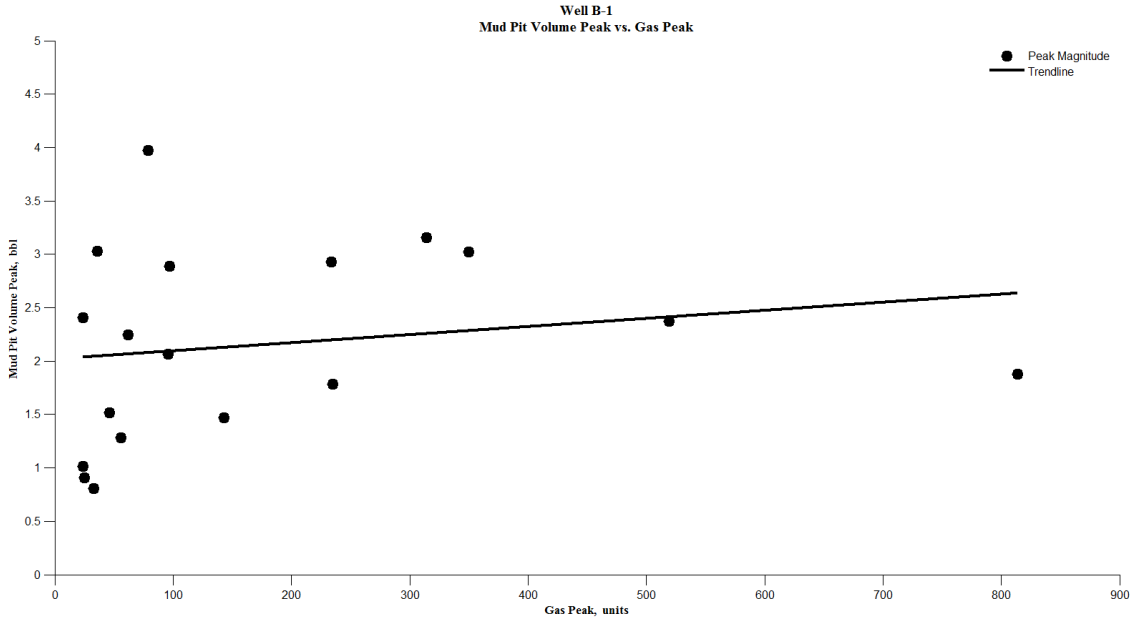

Figure 5.6 Cross-plot of mud pit volume peak vs. gas peak corresponding to each conductive natural fracture location identified for Well B-1.

A total of eleven conductive natural fracture zones have been identified for Well B-2 (see **Table 5.6 and Figure 5.7**). The zones are relatively evenly spaced over the lateral section. The natural fractures are estimated to have relatively high apertures ranging from 62 to 154 μm. In this case, the data seems to indicate a strong positive correlation between mud pit volume peak and gas peak (see **Figure 5.8**).

Table 5.6 Results from the natural fracture identification analysis for Well B-2.

Well B - 2					
Conductive Natural Fracture Location (ft)	**Aperture (μm)**	**Permeability (md)**	**Mud Pit Volume Peak (bbl)**	**Gas Peak (units)**	**Underbalance (psi)**
10680.3	87	1.45E+04	1.6	29	736
11081.2	76	1.27E+04	1.2	35	742
11102.9	122	2.03E+04	3.5	40	742
11428.3	73	1.22E+04	1.3	35	742
11541.9	66	1.10E+04	1.6	365	742
11874.5	78	1.30E+04	1.2	47	744
12824.6	73	1.22E+04	1.0	31	743
12957.8	136	2.27E+04	7.5	447	742
13012.3	76	1.27E+04	1.0	33	742
13072.0	73	1.22E+04	1.4	47	742
13627.1	62	1.03E+04	2.2	183	741
14158.6	154	2.57E+04	2.0	141	748

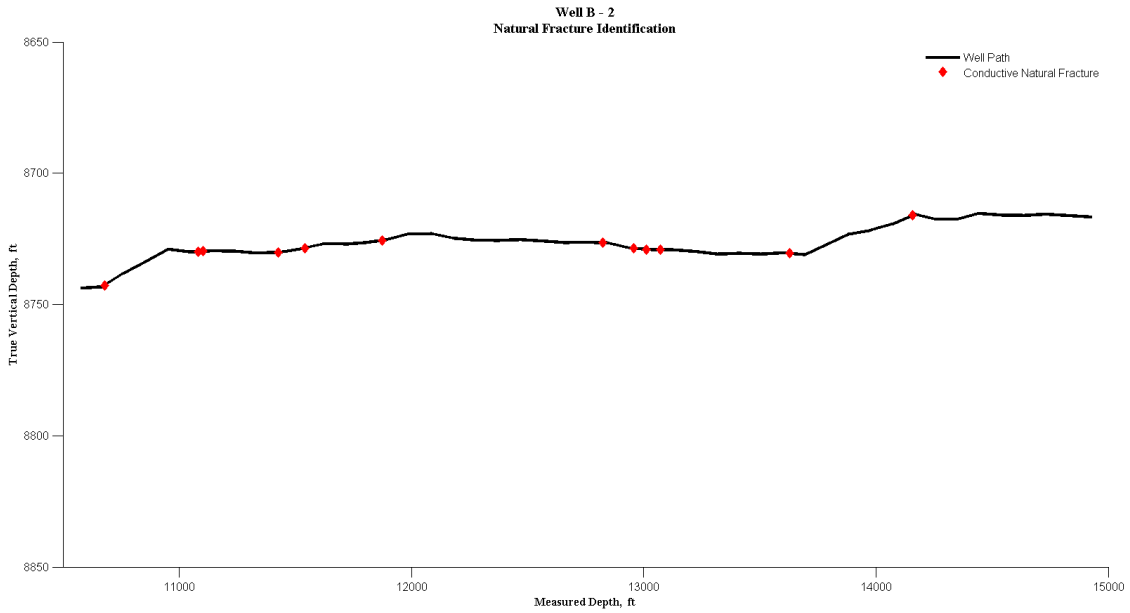

Figure 5.7 Locations of conductive natural fractures along the lateral of Well B-2.

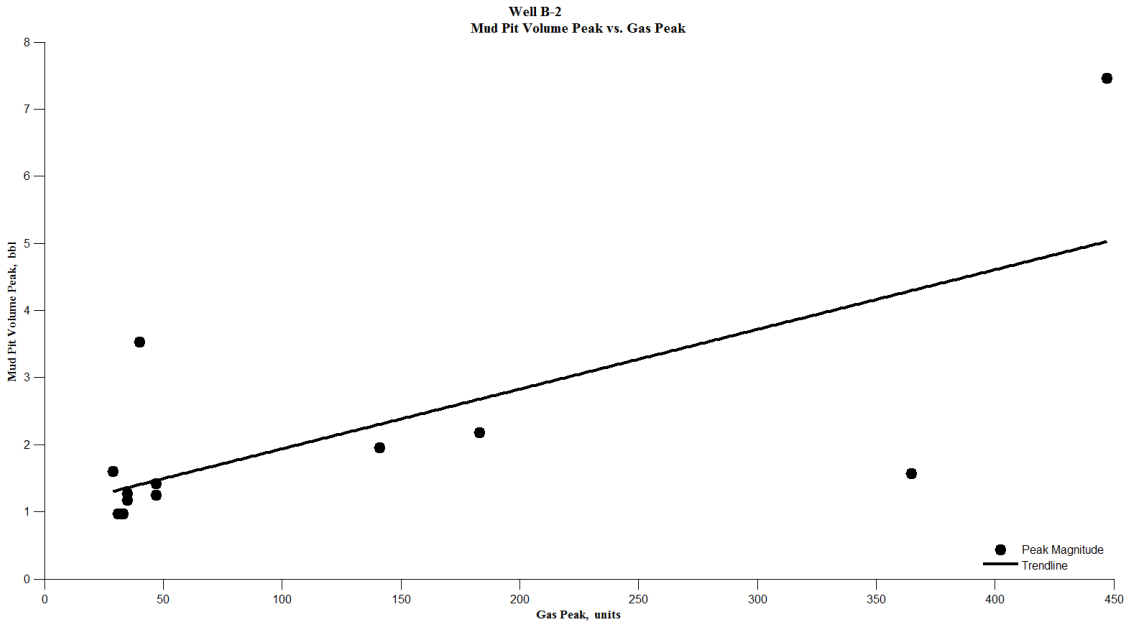

Figure 5.8 Cross-plot of mud pit volume peak vs. gas peak corresponding to each conductive natural fracture location identified for Well B-2.

A total of ten conductive natural fracture zones are identified for Well B-3 (see **Table 5.7 and Figure 5.9**). The majority of the zones are concentrated in the center of the lateral section. Two zones are located near the heel and three zones are located near the toe. Two large spans of the lateral contain no indications of conductive natural fractures. The estimated fracture apertures for these zones range from 36 to 114 μm. The cross-plot does not show much of a correlation at

all between mud pit volume peak and gas peak (see **Figure 5.10**). The trendline is heavily influenced by the single point associated with the fracture at a measured depth of 14,559.5' MD.

Table 5.7 Results from the natural fracture identification analysis for Well B-3.

Well B - 3					
Conductive Natural Fracture Location (ft)	**Aperture (µm)**	**Permeability (md)**	**Mud Pit Volume Peak (bbl)**	**Gas Peak (units)**	**Underbalance (psi)**
9929.0	66	3.63E+05	5.3	72	730
10023.5	67	3.74E+05	5.8	102	730
11640.3	98	8.00E+05	3.1	75	735
11878.5	64	3.41E+05	4.3	67	736
12004.4	103	8.84E+05	4.2	125	738
12099.6	67	3.74E+05	6.5	190	740
12355.5	83	5.74E+05	5.9	81	742
14514.3	36	1.08E+05	3.3	77	748
14559.5	114	1.08E+06	7.2	946	749
14735.4	90	6.75E+05	3.5	189	752

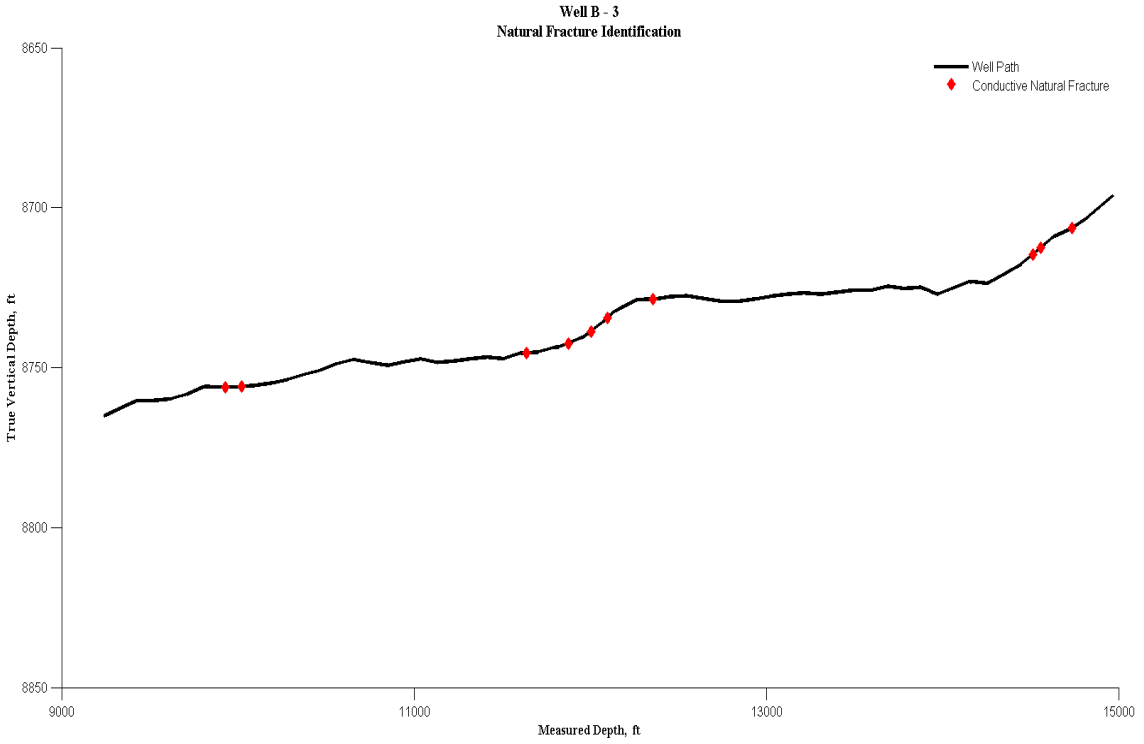

Figure 5.9 Locations of conductive natural fractures along the lateral of Well B-3.

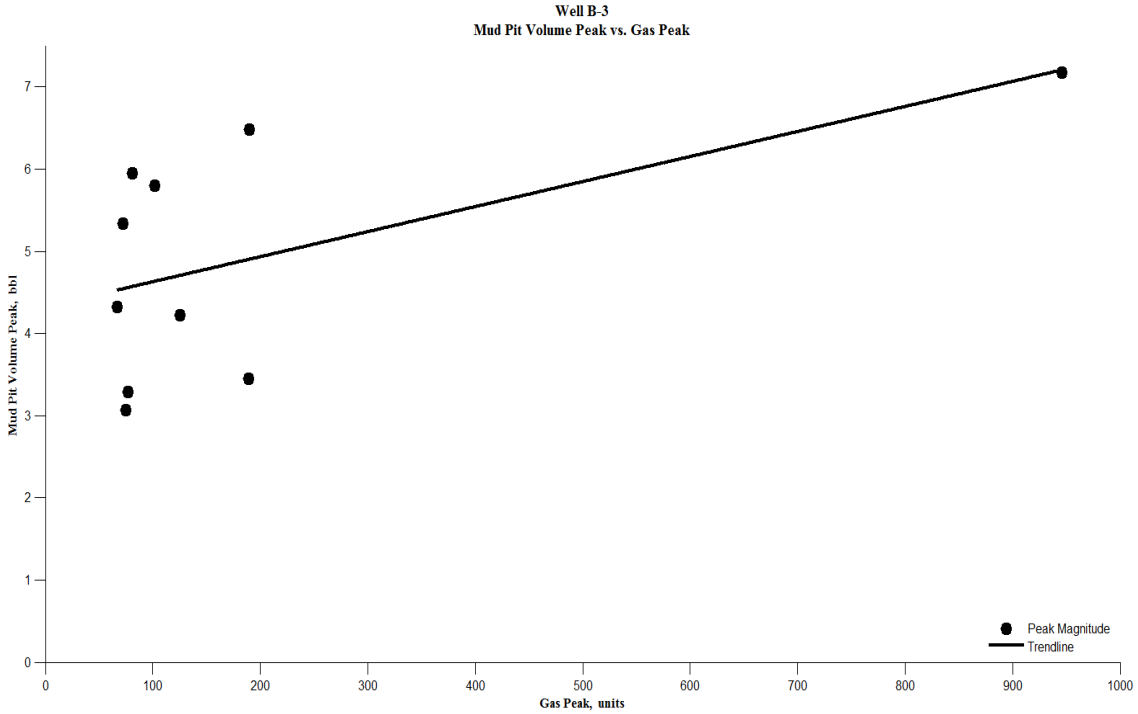

Figure 5.10 Cross-plot of mud pit volume peak vs. gas peak corresponding to each conductive natural fracture location identified for Well B-3.

Only six conductive natural fracture zones are identified for Well B-4 (see **Table 5.8 and Figure 5.11**). Three spans of the lateral contain no indications of conductive natural fractures: 10,000 to 11,000 ft, 11,750 to 12,500 ft, and 13,000 to 14,000 ft MD. Estimated fracture apertures range from 79 to 112 μm. The cross-plot indicates a weak positive correlation between mud pit volume peak and gas peak (see **Figure 5.12**).

Table 5.8 Results from the natural fracture identification analysis for Well B-4.

Well B - 4					
Conductive Natural Fracture Location (ft)	**Aperture (μm)**	**Permeability (md)**	**Mud Pit Volume Peak (bbl)**	**Gas Peak (units)**	**Underbalance (psi)**
11254.5	88	6.45E+05	3.9	87	732
11710.5	107	9.54E+05	4.8	52	733
12735.4	85	6.02E+05	5.3	71	740
14107.4	88	6.45E+05	4.0	82	741
14354.2	90	6.75E+05	4.5	80	740
14399.4	112	1.05E+06	4.4	50	740
14995.9	79	5.20E+05	5.7	132	742

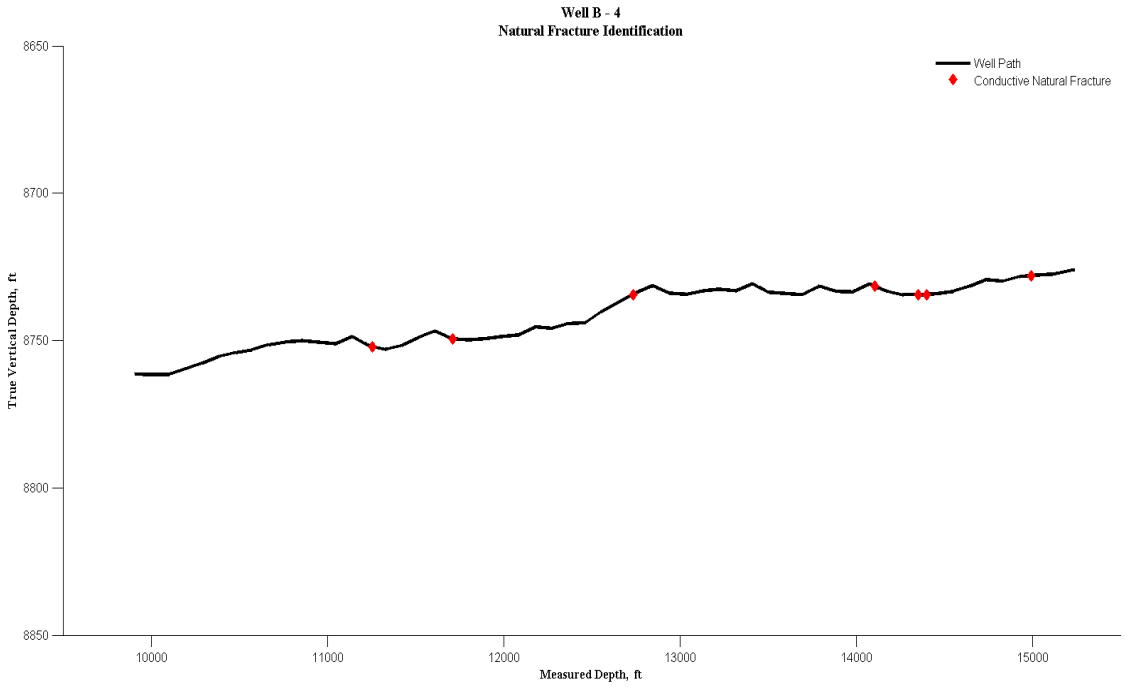

Figure 5.11 Locations of conductive natural fractures along the lateral of Well B-4.

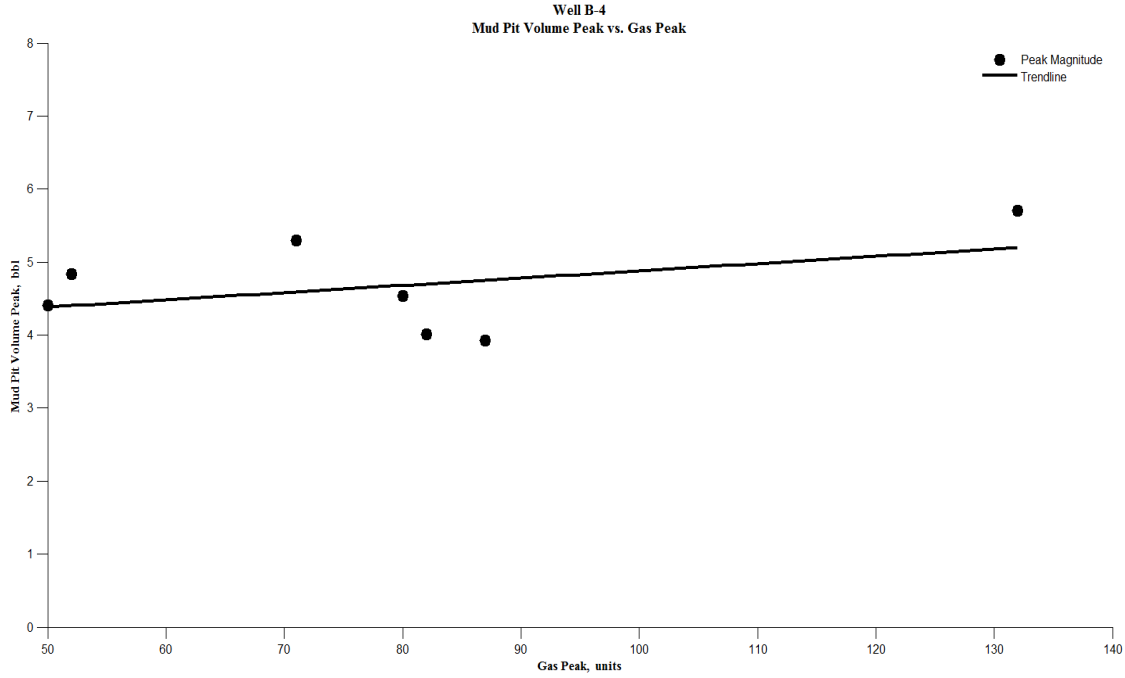

Figure 5.12 Cross-plot of mud pit volume peak vs. gas peak corresponding to each conductive natural fracture location identified for Well B-4.

5.2 Validation

No image logs are available for the data under investigation. An alternative method must be used to validate the results obtained in the previous section. These six wells have been selected for study specifically because they constitute three sets of parallel wells. In tight gas reservoirs it is common to drill wells in the direction believed to be perpendicular to the natural fracture system orientation. This practice ensures that the well will intersect the highest possible number of transverse natural fractures. Therefore, it is presumed that if two wells are drilled parallel to each other in close proximity there is a good chance they will penetrate similar natural fracture systems. The results of the natural fracture identification analysis from each set of parallel wells are compared.

Patterns in the locations of conductive natural fracture zones are considered an indication of the orientation of natural fracture planes. If the wells were truly drilled in the direction perpendicular to natural fracture system orientation, then conductive natural fracture locations of the parallel wells should pair up evenly on a plan view. If the natural fracture system is predominantly oriented in a different direction, the conductive natural fracture locations of parallel wells should pair up slightly offset. A consistent pattern of conductive natural fracture pairs is a strong indication that there is a physical basis for the results obtained in **Section 5.1**. This approach will be used to evaluate a confidence level for the methodologies developed in this thesis.

The measured depths of each well are transformed to a field-wide location (see **Figures 5.13 and 5.14**). The conductive natural fracture zones for each parallel well set are compared to determine if any dominant patterns are observed. If a pattern exists, the average orientation of the natural fracture system for the given field will be determined. It is important to remain objective when identifying natural fracture orientation patterns. While it is not assumed that natural fracture planes physically connect the two wells, it is conceivable that natural fractures along the same plane of weakness will have similar characteristics. Estimated fracture apertures of natural fracture zones that correspond to a unique natural fracture plane will be compared.

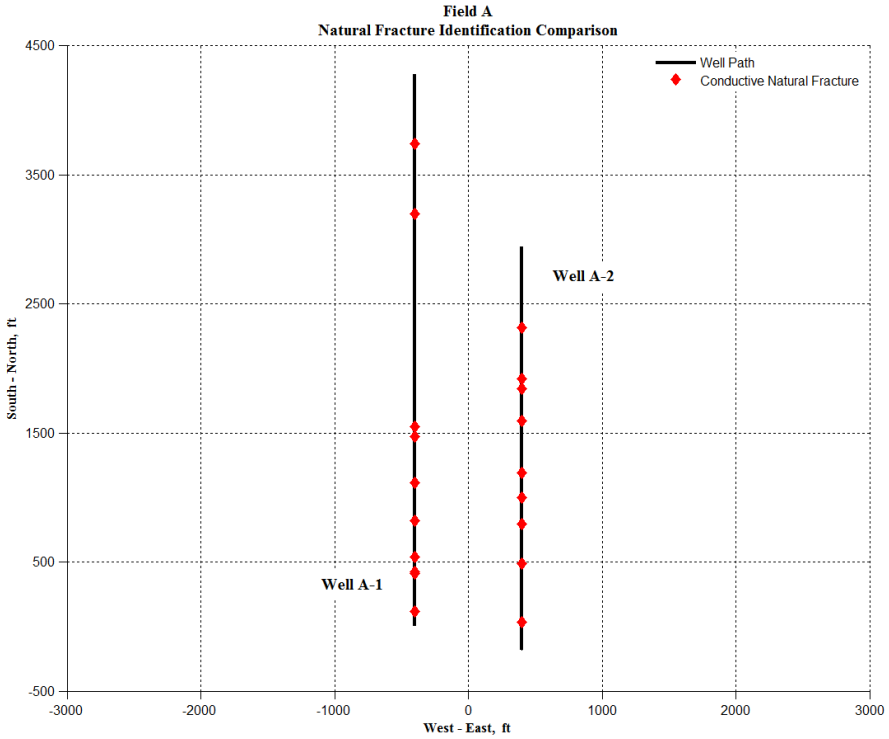

Figure 5.13 Plan view of Field A. Wells A-1 and A-2 are parallel wells drilled in the South – North direction. The lateral spacing between these wells is roughly 800 ft. Red diamonds indicate the locations of conductive natural fractures determined through the fracture identification analysis.

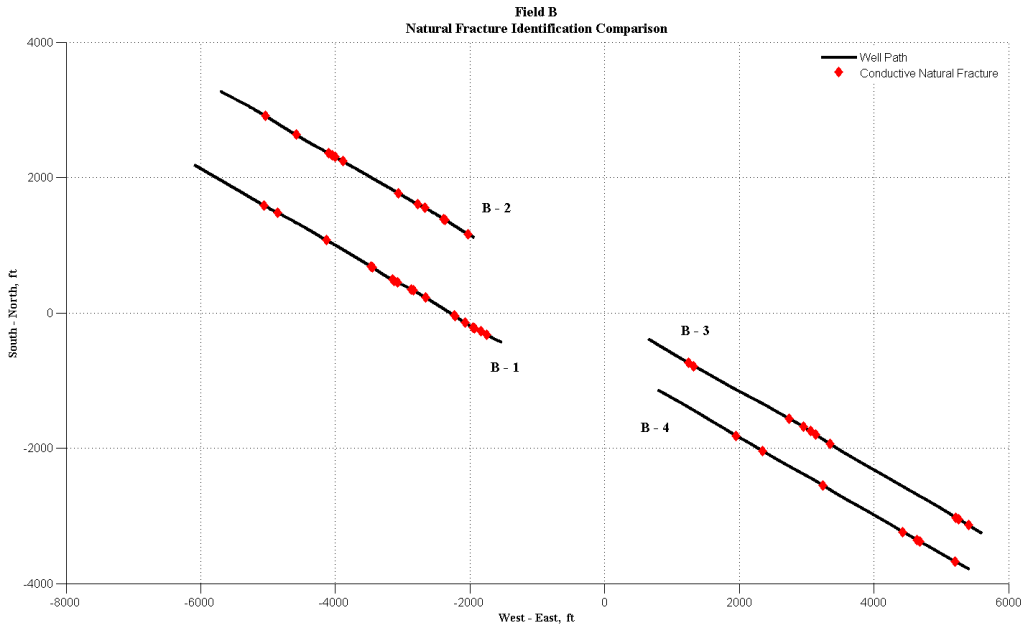

Figure 5.14 Plan view of Field B. These four wells were drilled from a common pad located near 0,0. Red diamonds indicate the locations of conductive natural fractures determined through the fracture identification analysis.

5.2.1 Field A

Consider the spans of Wells A-1 and A-2 that "overlap." Well A-1 contains seven natural fracture zones and Well A-2 contains nine. From visual inspection of **Figure 5.13** two dominant patterns are distinguished. Orientation #1 is illustrated in **Figure 5.15**. This orientation is the stronger of the two patterns. Of the possible 16 natural fracture zones between the two wells, 14 zones constitute "pairs" of natural fractures aligned at similar orientation. Upon further examination, it is clear that only one natural fracture zone from Well A-2 does not have a corresponding zone in Well A-1. If Orientation #1 is accepted as the natural fracture system orientation for Field A, then it is unfair to include the most southern natural fracture zone from Well A-2 in this comparison because Well A-1 does not extend far enough South to draw any conclusions.

Orientation #1 suggests that these two wells intersect a minimum of seven natural fracture planes. The average orientation of the suggested natural fracture planes is N65°E. The results of the fracture aperture comparison study for this orientation are portrayed in **Table 5.9**. With the exception of Pair #4 and Pair #5 (numbered from North to South), the estimated fracture apertures agree relatively well.

Orientation #2, illustrated in **Figure 5.16**, suggests that these wells intersect a minimum of four natural fracture planes. The average orientation of the suggested natural fracture planes is N84°E. The results of the fracture aperture comparison study for this orientation are portrayed in **Table 5.10**. Estimated fracture apertures for these pairs do not seem to agree well.

Table 5.9 Comparison of estimated fracture aperture between "pairs" of conductive natural fractures for Wells A-1 and A-2. These pairs assume Orientation #1. Pairs are numbered from North to South.

Orientation #1		
Pair #	**(μm)**	**(μm)**
1	42	29
2	36	32
3	37	38
4	42	16
5	44	15
6	44	34
7	30	25
Average	39	27

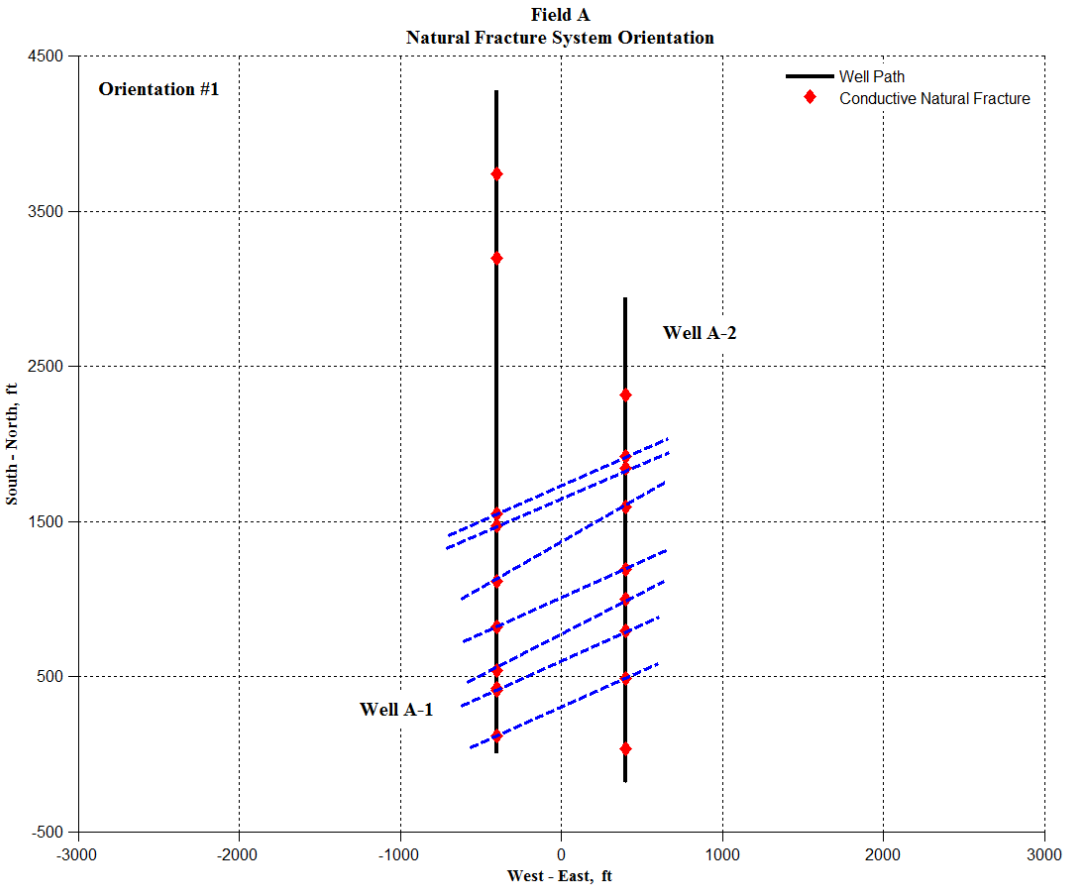

Figure 5.15 Natural Fracture System Orientation #1 for Field A. A dominant pattern exists that seems to indicate the presence of a natural fracture system oriented at N65°E.

Table 5.10 Comparison of estimated fracture aperture between "pairs" of conductive natural fractures for Wells A-1 and A-2. These pairs assume Orientation #2. Pairs are numbered from North to South.

Orientation #2		
Pair #	**(µm)**	**(µm)**
1	39	38
2	37	16
3	42	15
4	44	25
Average	41	24

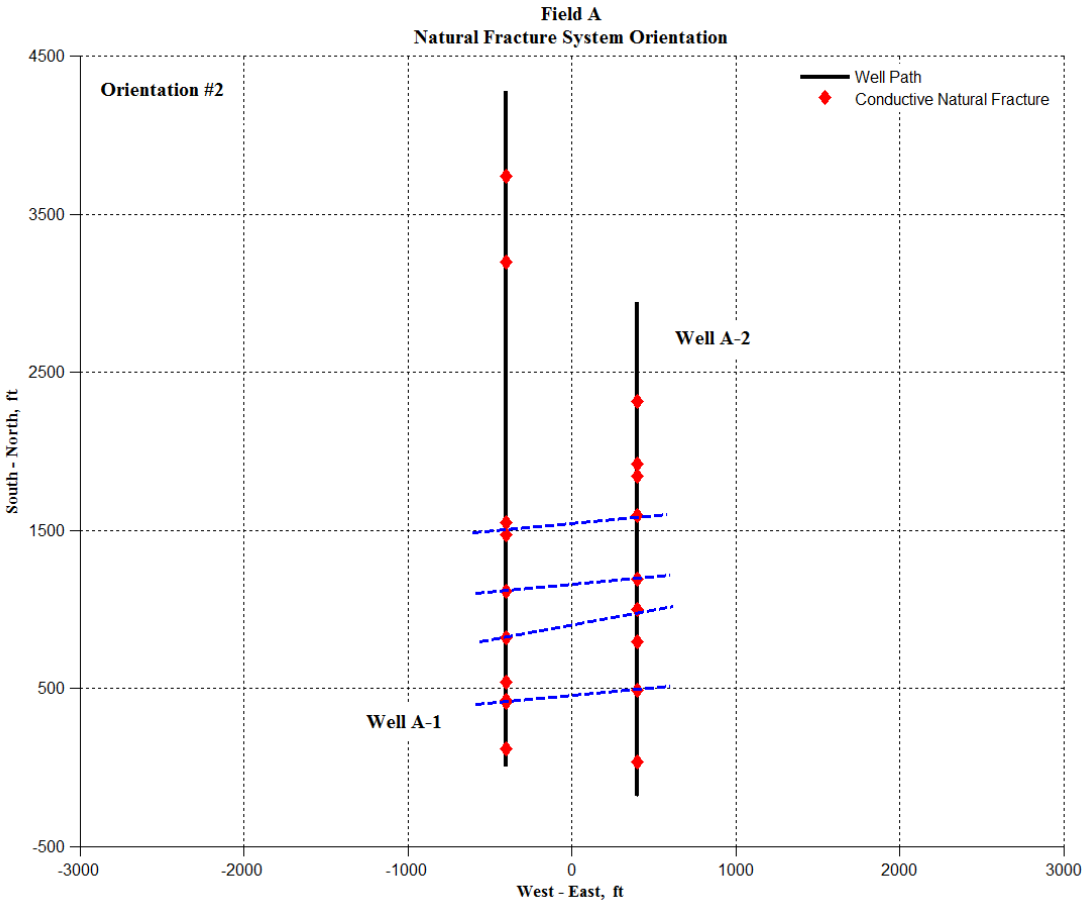

Figure 5.16 Natural Fracture System Orientation #2 for Field A. A moderate pattern exists that seems to indicate the presence of a natural fracture system oriented at N84°E.

5.2.2 Field B

Field B consists of two parallel well sets. Wells B-1 and B-2 were drilled in the opposite direction as Wells B-3 and B-4. A field-wide comparison is made to determine if any patterns exist that would seem to indicate natural fracture planes (see **Figure 5.14**). In general, it is observed that the natural fracture zones identified for Wells B-3 and B-4 do not display many strong patterns. Wells B-1 and B-2, however, display two distinct patterns.

Orientation #1 suggests that Wells B-1 and B-2 intersect seven natural fracture planes, and Wells B-3 and B-4 intersect two planes (see **Figure 5.17**). The average orientation of the suggested natural fracture planes is N12.5°E. First, consider the "overlapping" spans of Wells B-1 and B-2. Four natural fracture zones do not have a corresponding zone in the other well. In contrast, 14 natural fracture zones constitute pairs. Now consider the "overlapping" spans of Wells B-3 and B-4. Out of the total number of natural fracture zones identified for these two

wells, 12, four zones constitute pairs while eight zones do not have a corresponding match. The results of the fracture aperture comparison study for Orientation #1 are given in **Table 5.11**.

Orientation #2 suggests that Wells B-1 and B-2 intersect a minimum of six natural fracture planes, and Wells B-3 and B-4 intersect a minimum of one plane (see **Figure 5.18**). The average orientation of the suggested natural fracture planes is N2°E. First, consider Wells B-1 and B-2. Of the total number of identified natural fracture locations, 18, there are 12 fractures that have a corresponding match in the other well. Now, consider Wells B-3 and B-4. Only one pair exists at this orientation out of the possible 12 identified natural fractures. The results of the fracture aperture comparison study for Orientation #2 are given in **Table 5.12**.

Table 5.11 Comparison of estimated fracture aperture between "pairs" of conductive natural fractures for all wells in Field B. These pairs assume Orientation #1. Pairs are numbered from West to East.

Orientation #1		
Pair #	**North Well Aperture (µm)**	**South Well Aperture (µm)**
1	53	62
2	53	73
3	88	78
4	112	66
5	79	73
6	76	99
7	85	87
8	83	85
9	114	79
Average	83	78

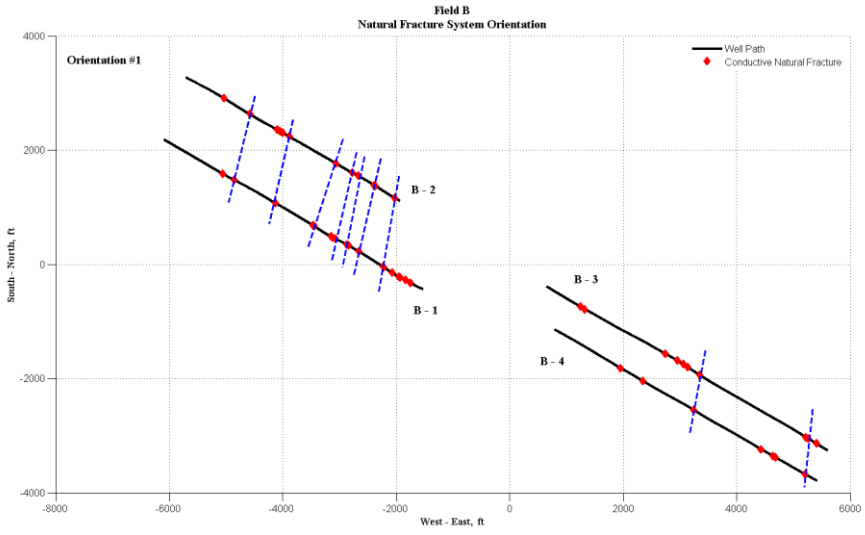

Figure 5.17 Natural Fracture System Orientation #1 for Field B. A strong pattern exists that seems to indicate the presence of a natural fracture system oriented at N12.5°E.

Table 5.12 Comparison of estimated fracture aperture between "pairs" of conductive natural fractures for all wells in Field B. These pairs assume Orientation #2. Pairs are numbered from West to East.

Orientation #2		
Pair #	**North Well Aperture (µm)**	**South Well Aperture (µm)**
1	73	154
2	53	76
3	97	78
4	79	66
5	76	73
6	99	87
7	75	79
Average	79	88

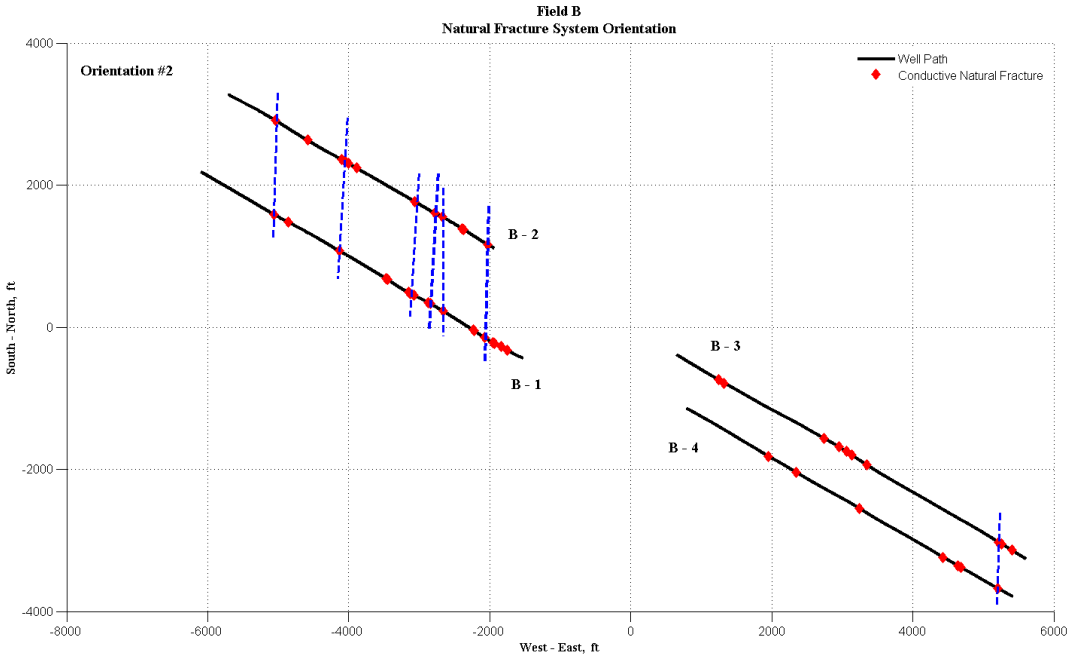

Figure 5.18 Natural Fracture System Orientation #2 for Field B. A moderately strong pattern exists that seems to indicate the presence of a natural fracture system oriented at N2°E.

CHAPTER 6: DISCUSSION AND FUTURE WORK

6.1 Introduction

A total of six wells in tight gas reservoirs that were drilled underbalanced have been analyzed. Conductive natural fracture zones have been identified for each well and the permeability of each zone has been estimated. Several techniques used to validate the results have been implemented. The results of the study are presented in **Chapter 5**. In this chapter, the results will be interpreted. Based upon the validation study the author's level of confidence in the methodologies is moderate to high and future research is warranted. Future areas of research related to this topic are discussed.

6.1.1 Natural Fracture Identification and Characterization

The natural fracture identification and characterization analysis has been performed on six wells from tight gas reservoirs that were drilled underbalanced. On average, the computational tool identifies between nine and ten conductive natural fracture zones for each well. The true number of natural fractures that intersect each well is unknown, but focusing on roughly ten zones seems to be a practical target in terms of hydraulic fracture treatment designs. Identifying too many zones may not provide a helpful sense of the most productive zones along the wellbore, whereas identifying too few zones may not give engineers confidence in the results.

For each conductive natural fracture zone, the fracture aperture and fracture permeability has been estimated. The estimated fracture apertures all lie within the expected range of values (i.e., 10 to 1000 μm). This is very encouraging, because several non-trivial assumptions were made in order to estimate fracture aperture. The true level of underbalance at any location along the wellbore is generally unknown because the downhole drilling mud pressure and reservoir pore pressure profiles are not measured directly. However, it was discussed in **Section 4.2.3** that the method used in this research for determining bottomhole pressure leads to a conservative estimate of fracture aperture. In addition, estimates of gas flow rate through each fracture are based on the mud pit volume response. This is a major assumption that neglects several important considerations. Pressure and temperature will play a key role once the gas bubble has left the fracture and entered the stream of circulating drilling fluid. The volume of space in the annulus occupied by the gas bubble, and therefore the mud pit volume response, is largely influenced by the high compressibility of gas. Reports have indicated that natural gas is highly soluble in oil-based mud, which was the type of mud used to drill all six of the wells investigated in this study. As a consequence, the true mud pit volume response to a gas influx will be masked by a smaller

magnitude spike. This observation also leads to a conservative estimate of fracture aperture. In summary, although the estimates of fracture aperture may not be entirely accurate, they should be considered as a lower-bound for the true fracture apertures.

The fracture identification criteria are based on observations of mud pit volume and total gas concentration. Comparisons between mud pit volume peak and gas peak at each conductive fracture location for each well have been presented. In theory, the magnitudes of these two responses should have a positive correlation. The cross-plots presented in **Section 5.1** are used to validate this hypothesis. Overall, the quality of the results from this portion of the study is moderate, but acceptable. Each cross-plot does indeed show a positive correlation, as expected. Cross-plots for Well A-1, Well B-2, and Well B-4 show moderate to strong correlations with consistent data. The remainder of the wells, while exhibiting a positive correlation, do not display data that garners a high level of confidence. For example, in **Figure 5.10** it is observed that the trendline is highly influenced by a single point of relatively high mud pit volume peak and gas peak magnitude. The other data points do not seem to suggest a strong correlation. However, it should be noted that the identified natural fracture zones have passed a rigorous set of screening criteria as well as engineering judgment, and based on the drilling and mud logs there is no reason to exclude any of the locations determined through the analysis. Due to the high level of noise present in the data and uncertainty in the methodologies, the fact that all cross-plots indicate a positive correlation is considered encouraging. Nonetheless, it is not recommended that this data set be used to establish any type of empirical relationship between mud pit volume response and total gas concentration response.

6.1.2 Validation

Three sets of parallel wells are considered for this study. The results of the natural fracture identification and characterization analysis for each pair of wells are compared. It is argued that patterns in the locations of conductive natural fracture zones between wells could be a means to validate the results because each pair of wells should penetrate similar geologic conditions. In addition, patterns could indicate the orientation of the natural fracture system in each region. Overall, the results of the validation analysis are encouraging. Two out of the three parallel well pairs exhibit strong patterns. If the orientation of the natural fracture system has been determined from geologic data, then the results could be further validated and the confidence level in the proposed methodologies would be greatly enhanced.

From visual inspection of the results obtained for Field A two dominant patterns can be observed (see **Figure 5.13**). A total of seven pairs of natural fractures are aligned at an orientation of roughly N65°E (see **Figure 5.15**). Only one identified natural fracture from Well A-2 does not have a corresponding feature in Well A-1. For each of the seven natural fracture planes identified, the estimated apertures of the corresponding pair of natural fractures compare well, with the exception of Pairs 4 and 5 (see **Table 5.9**). In order to remain objective, more than one pattern orientation must be considered. For Field A, an alternate orientation is observed at which four pairs of natural fractures are aligned at roughly N84°E (see **Figure 5.16**). The pattern in Orientation #2 is clearly not as strong in Orientation #1. The correlation between estimated fracture apertures in Orientation #2 is not as strong as Orientation #1 (see **Table 5.10**). If the results of this investigation are to be trusted, Orientation #1 is recommended to be considered representative of the natural fracture system in Field A.

From visual inspection of the results obtained for Field B a dominant pattern is observed between Wells B-1 and B-2, and a weak pattern is observed between Wells B-3 and B-4 (see **Figure 5.14**). A total of nine pairs of natural fractures align at the orientation of roughly N12.5°E across the four wells (see **Figure 5.17**). For each of the nine identified natural fracture planes, the estimated apertures of the corresponding fracture pair agree quite well (see **Table 5.11**). A second pattern is observed for Field B, corresponding to an orientation of N2°E (see **Figure 5.18**). A total of seven natural fracture planes are identified assuming this orientation. The estimated fracture apertures of these seven pairs of fractures agree relatively well, with the exception of Pair #1 (see **Table 5.12**).

Please note that no physical connection is implied to exist between pairs of fractures associated with a common fracture plane. The motivation behind these comparisons is that for a given in-situ horizontal stress distribution natural fractures will tend to develop along a particular orientation. It is reasonable to assume that multiple natural fractures will develop along the same line of action in a given region.

The purpose of this study is to develop methodologies that are helpful in gaining information about the natural fracture spacing along the wellbore, the permeability of conductive fractures intersected by the wellbore, and the natural fracture system orientation. In order to demonstrate the practicality of the techniques, the methodologies have been implemented to characterize the natural fracture system in six existing wells in tight gas reservoirs. A validation analysis has been performed to develop a sense of confidence in the proposed methodologies

because no other methods are currently available to identify the true locations of natural fractures downhole in these six wells. As it stands, the confidence level in the proposed technique is moderate to high. In two of the three parallel well pairs considered, the application of several fracture identification criteria based upon physical processes has provided a strong indication of the presence of a natural fracture system.

6.2 Future Work

This report represents one of the first of its kind to propose methodologies to characterize natural fracture systems making use only of data that is recorded during underbalanced drilling operations. The project has been industry-driven, with practical implementation as a topmost priority. As such, the types of data considered and the analysis techniques employed have been subject to certain constraints that act to limit the accuracy of the results. This study seeks to set precedence for future research that aims to exploit inexpensive underbalanced drilling data for the purposes of natural fracture characterization. In this section, several suggestions are made to direct future research projects related to this topic.

One of the main issues addressed in this study is the fact that, in the absence of any other data, the results of the fracture identification analysis are dubious because the true geometry of the natural fracture system is unknown. Without any previous experience published in this type of work, it is difficult for an engineer to genuinely believe the results of natural fracture locations subject to the fracture identification criteria described in this report. A validation approach making use of wells there were drilled in parallel attempts to quantify the level of confidence in the results for the six wells used in this study. However, if the required data is available, several additional validation tests could be applied towards this type of analysis. The most obvious option is to compare the results to optical, acoustic, or resistivity image logs. This is potentially the most accurate validation technique, provided that the resolution quality of the image log is sufficient to identify the productive features. In many cases, geologic knowledge of a site is well known before drilling commences. Predictions or estimates of the in-situ stress conditions aid in determining the optimal drilling path. The in-situ stress condition (past and present) determines the orientation of the natural fracture system of the site. In fact, drilling engineers orient the horizontal section of wells drilled in tight gas reservoirs in the direction that will intersect the largest number of natural fractures. If this type of detailed geologic information is known about a particular site, then the validation approach described in this thesis becomes even more effective. Recent advances in 3-D seismic technology have produced techniques for delineating natural fracture systems, which could be compared with the results from the technique proposed in this

thesis. Lastly, microseismic monitoring during hydraulic fracture treatments provides another method to evaluate the results of the proposed methodologies. The early-time events recorded during pad fluid injection are often attributed to existing natural fractures that effectively re-open during initial injection. The location of these types of events could be compared to the fracture identification analysis results.

For the purposes of the present research, conductive natural fracture zones are identified at locations where simultaneous "large" peaks in the mud pit volume and total gas concentration are observed. More fracture identification criteria could be applied to increase the user's confidence level. For example, it is well known that when a fracture is intersected by the wellbore during conventional overbalanced drilling operations the bottomhole pressure decreases as fluid is lost into the fracture. A unique downhole pressure response is likely to occur in the reverse case during underbalanced drilling, as gas influx rapidly enters the wellbore. While it is not common to obtain direct downhole pressure measurements during drilling at this time, the technology does exists to place pressure sensors downhole to record a continuous downhole pressure profile during drilling. Investigation into the type of bottomhole pressure response that is to be expected as a natural fracture is intersected at underbalanced conditions would be very beneficial to the industry. Similar investigations could be implemented to determine the response of ROP or WOB to a natural fracture. Contracting the mud logger to record the locations where sudden gas peaks occur would aid in the identification of sweet spots. Additionally, the computational routine used to define the appropriate magnitude of peak to be highlighted deserves discussion. A statistical approach based on the average noise level in the data is used to determine the appropriate cut off level for mud pit volume peak and gas peak. A more sophisticated approach for processing the data would take account for the high coefficient of variation observed in the data sets used in this study, i.e. typically ≥ 1. It is recommended to investigate the possibility of mud pit volume peaks and gas peaks exhibiting a log-normal distribution.

The model used in this study to estimate fracture aperture is the cubic law for fracture flow. The estimates reported in this study have been shown to be conservative, however, the accuracy of these estimates could be enhanced through consideration of the following concepts. First and foremost, direct measurements of gas flow rate should be recorded if at all possible. Research into advanced methods for separating produced gas from the drilling fluid stream would be greatly beneficial to this type of project. Correlations between total gas concentration and gas flow rate would be helpful to compare with observations of mud pit volume if gas influx rate

cannot be measured directly. Further study into the effects of gas solubility in oil-based mud and PVT relationships in wellbore conditions are necessary to improve gas influx rate estimates based on data that is currently available. Precise measurements of downhole drilling fluid pressure and reservoir pore pressure profiles are helpful to classify the level of underbalance. Finally, a numerical model that considers transient flow of a highly compressible gas through fractured media would certainly be a useful tool to obtain more accurate estimates of fracture aperture.

CHAPTER 7: CONCLUDING REMARKS

Fluid flow through the fracture network is known to dominate production from unconventional, low permeability oil and gas reservoirs. In many deep tight gas reservoirs it is expected that the natural fracture system is predominantly comprised of vertical fractures. In order to intersect the maximum number of natural fractures, it has therefore become common practice to drill horizontal wellbores in these types of reservoirs. Among other technical advantages, it has been recognized that drilling underbalanced greatly enhances the rate of penetration; in many cases the lateral section of horizontal wellbores are drilled underbalanced to reduce drilling costs. The downhole pressure condition while drilling underbalanced has the consequence of inducing hydrocarbon production throughout the drilling process. Experience has shown that if the production rate can be accurately determined, then information about the reservoir properties such as formation permeability and pore pressure can be determined, similar to pressure transient testing. This thesis describes an approach to identify and characterize the permeability of natural fractures that are intersected by the wellbore using data that can be obtained during underbalanced drilling operations.

The project is industry-oriented and the practical application of the methodologies developed within this thesis has been a primary consideration. The investigation discussed within this thesis is essentially an exploitation study to use data that is commonly recorded for every new well that is drilled underbalanced to gain useful information about the natural fracture system present near-wellbore. Properties of the natural fracture system near-wellbore, such as fracture spacing, permeability, and orientation, have extreme economic implications from the perspective of the hydraulic fracture treatment design.

For the purposes of this study, two pieces of data recorded during drilling operations have been identified as having a physical basis for indicating the presence of natural fractures: mud pit volume measurements and total gas concentration measurements. The premise behind this physical basis is that as a natural fracture is intersected by the wellbore while the underbalance pressure condition exists, the volume of gas originally contained within the fracture will rapidly flow into the wellbore. As opposed to a normal gas kick situation, this phenomenon is primarily due to the extremely high permeability of the fracture and in general is not considered unsafe. As the gas enters the wellbore, it will displace a volume of the drilling fluid which is observable at the surface. In addition, as the drilling fluid circulates back to the surface a noticeable “spike” should appear on the mud log. Current mud logging practice accounts for the circulation lag time, and an accurate position along the wellbore at which the gas influx originally occurred can be

determined. It is plausible that a natural fracture exists at the location along the wellbore where these two events occur simultaneously.

A computational tool has been developed that processes the drilling and mud log data from wells that were drilled underbalanced. Spikes in both mud pit volume and total gas concentration are used as fracture identification criteria. A threshold can be set by the user to quantify an appropriate magnitude of spike that serves to distinguish a response to a natural fracture from random noise in the data. The input data can be prepared in a relatively short time frame (i.e., less than a day) and the analysis can then be performed immediately. In theory, this type of analysis could actually be performed in near real-time as the well is being drilled. The results from the analysis indicate the zones along the wellbore at which the presence of a natural fracture is highly probable. The effective fracture permeability is estimated for each zone that is identified using estimates of gas influx rate.

The approach described within this thesis has been applied to six data sets from horizontal wells that were drilled underbalanced in tight gas reservoirs. The wells consist of three sets of parallel well pairs. No information was provided by the sponsor about the natural fracture systems in the fields considered in this study that would help to prove the existence of the identified natural fractures (i.e., FMI logs, in-situ stress condition, geologic history). In an attempt to quantify the level of confidence in the proposed methodologies the results from the analysis are compared for each pair of parallel wells. It is argued that patterns in the locations of conductive natural fractures in parallel wells could be an indication of the presence of the natural fracture system in the region. In two of the three well pairs considered, the majority of identified conductive fracture locations in one well aligned with a corresponding feature in the parallel well. Based on these comparisons, the author's confidence level in these methodologies is moderate to high. The methodologies warrant further research.

This study provides a foundation for future studies on the topic of natural fracture characterization using data that can be obtained during underbalanced drilling operations. Many basic assumptions were made in this analysis because of practical considerations. As experience is gained in this area many of these assumptions could be relaxed. Improvements to this analysis could be made to enhance the accuracy of the natural fracture identification procedure and estimates of natural fracture permeability. In particular, the most critical component of this type of analysis is the measurement of the rate of produced fluids; industrial research into effective techniques for measuring fluid production rate throughout the drilling process is essential to

progress the effort to use underbalanced drilling data for the purposes of natural fracture characterization. Furthermore, it is recommended to include any additional types of data recorded on individual drilling rigs that would serve as fracture identification criteria in order to bolster confidence in the fracture identification procedure. Finally, if any means exist to further validate the proposed methodologies, then they should be exploited. The framework has been presented and can be easily updated as further insight into the problem is achieved.

This thesis presents a novel method to characterize natural fracture systems using inexpensive data. At this time, sound engineering judgment must be exercised while interpreting the results of the analysis. The economic implications of this type of work are yet to be seen, but the results obtained from this analysis could have potentially large impacts on the practice of hydraulic fracture treatment design.

NOTATION

b	Constant used for Arps' decline-curve analysis method, [dimensionless]
C	Constant used in cubic law relationship, $\left[L^{-1}t^{-1}\right]$
c_t	Total compressibility; equal to the sum of fluid and pore compressibility, $\left[L^2/F\right]$
D_i	Constant used for Arps' decline-curve analysis method, $\left[t^{-1}\right]$
D_{MD}	Measured depth, $\left[L\right]$
D_{TVD}	True vertical depth, $\left[L\right]$
g	Gravitational constant, $\left[L/t^2\right]$
G	Total gas concentration, $\left[units\right]$
h	Hydraulic head, $\left[L\right]$
k	Permeability, $\left[L^2\right]$
k_f	Fracture permeability, $\left[L^2\right]$
L	Sample length for Darcy experiment, $\left[L\right]$
M	Measurement of interest; either mud pit volume peak or gas peak, $\left[L^3\right]$ or $\left[units\right]$
n	Total number of rows of data in drilling and mud log data, [dimensionless]
N	Standard deviation coefficient, [dimensionless]
P	Pressure, $\left[F/L^2\right]$
P_{BHP}	Bottomhole pressure, $\left[F/L^2\right]$
P_{DHP}	Downhole pressure of drilling fluid, $\left[F/L^2\right]$

P_{res} Reservoir pore pressure, $\left[F/L^2\right]$

ΔP_{ann} Frictional pressure loss in the annulus during drilling fluid circulation, $\left[F/L^2\right]$

ΔP_{OB} Overbalance pressure, $\left[F/L^2\right]$

ΔP_{UB} Underbalance pressure, $\left[F/L^2\right]$

q Cumulative production, $\left[L^3\right]$

$\dot{q}$ Production rate, $\left[L^3/t\right]$

$\dot{q}_i$ Initial production rate, $\left[L^3/t\right]$

Q Fluid flow rate, $\left[L^3/t\right]$

Q_{gas} Influx rate of gas from fracture into wellbore during underbalanced drilling, $\left[L^3/t\right]$

r Radius, $\left[L\right]$

R Rate of penetration, $\left[L/t\right]$

R_e Radial extent of fracture, $\left[L\right]$

R_w Wellbore radius, $\left[L\right]$

t Time, $\left[t\right]$

$\vec{v}$ Darcy fluid velocity in three dimensions, $\left[L/t\right]$

v Darcy fluid velocity in one dimension, $\left[L/t\right]$

v_m Velocity of drilling mud invasion front, $\left[L/t\right]$

$\left(V_m\right)_{\max}$ Maximum mud loss volume, $\left[L^3\right]$

V_{pit} Mud pit volume, $\left[L^3\right]$

w Fracture aperture, $[L]$

X Mud pit volume level or total gas concentration, $[L^3]$ or $[units]$

Greek Symbols

β Inertial factor for non-Darcy flow, $[L^{-1}]$

γ_{mud} Unit weight of drilling mud; mud weight gradient, $[F/L^3]$

κ Hydraulic conductivity, $[L/t]$

μ Fluid viscosity, $[F \cdot t/L^2]$

μ_M Average of measurement of interest, $[L^3]$ or $[units]$

μ_p Plastic viscosity for non-Newtonian fluid, $[F \cdot t/L^2]$

π Pi, dimensionless

ρ Fluid density, $[M/L^3]$

σ_M Standard deviation of measurement of interest, $[L^3]$ or $[units]$

τ_y Yield stress for non-Newtonian fluid, $[F/L^2]$

ϕ Porosity, [dimensionless]

GLOSSARY

AFIT:	Acoustic formation imaging technology – type of image log
BEM:	Boundary element method
BHP:	Bottomhole pressure
Bottomhole:	Used to refer to the location of the drillbit during drilling
Connection Gas Event:	Mechanically induced "spike" in the total gas concentration that appears on the mud log after each drillstring connection is made
DCA:	Decline-curve analysis
DFIT:	Diagnostic fracture injection test analysis which can be used to estimate formation pore pressure
Downhole:	Used to refer to an arbitrary location along the wellbore during drilling, not necessarily at bottomhole (see Bottomhole)
EUR:	Estimated ultimate recovery
FMI:	Formation micro-image – type resistivity of image log
Gas Peak:	The observed increase in total gas concentration on the mud log as a natural fracture is intersected by the wellbore
MD:	Measured depth
MPD:	Managed pressure drilling
Mud Pit Volume Peak:	The observed increase in mud pit volume as a natural fracture is intersected by the wellbore
OGIP:	Original gas in place
ROP:	Rate of penetration
TCM:	Type-curve matching
Tight Gas Reservoir:	Natural gas reservoir with matrix permeability less than 0.1 md
TVD:	True vertical depth
UBD:	Underbalanced drilling
WOB:	Weight on bit

REFERENCES

Agarwal, R.G., Carter, R.D., and Pollock, C.B. 1979. Evaluation and Performance Prediction of Low-Permeability Gas Wells Stimulated by Massive Hydraulic Fracturing. *J Pet Technol* (March 1979) 362-372.

Aguilera, R. 2008. Role of Natural Fractures and Slot Porosity on Tight Gas Sands. Paper SPE 114174 presented at the 2008 SPE Unconventional Reservoirs Conference, Keystone, Colorado, USA, 10-12 February. doi: 10.2118/114174-MS.

Anderson, D.M., Nobakht, M., Moghadam, S., and Mattar, L. 2010. Analysis of Production Data from Fractured Shale Gas Wells. Paper SPE 131787 presented at the 2010 SPE Unconventional Gas Conference, Pittsburgh, Pennsylvania, USA, 23-25 February. doi: 10.2118/131787-MS.

Aremu, O.J., and Osisanya, S.O. 2008. Reduction of Wellbore Effects on Gas Inflow Evaluation Under Underbalanced Conditions. *SPE Journal* **13** (2):216-225. SPE 91586-PA. doi: 10.2118/91586-PA.

Arps, J.J. 1945. Analysis of Decline Curves. Trans., AIME, **160**: 228-247.

Barton, C.A., and Zoback, M.D. 2002. Discrimination of Natural Fractures From Drilling-Induced Wellbore Failures in Wellbore Image Data – Implication for Reservoir Permeability. *SPE Res Eval & Eng* **5** (3): 249-254. SPE 78599-PA. doi: 10.2118/78599-PA.

Basquet, R., Jeannin, L., Lange, A., Bourbiaux, B., and Sarda, S. 2004. Gas-Flow Simulation in Discrete Fracture-Network Models. *SPE Res Eval & Eng* **7** (5): 378-384. SPE 88985-PA. doi: 10.2118/88985-PA.

Biswas., D., Suryanarayana, P.V., Frink, P.J., and Rahman, S. 2003. An Improved Model to Predict Reservoir Characteristics During Underbalanced Drilling. Paper SPE 84176 presented at the 2003 SPE Annual Technical Conference and Exhibition, Denver, Colorado, USA, 5-8 October. doi: 10.2118/84176-MS.

Carter, R.D. 1985. Type Curves for Finite Radial and Linear Gas-Flow Systems: Constant-Terminal-Pressure Case. *SPE J.* (October 1985) 719-728.

Chen, Z., Narayan, S.P., Yang, Z., and Rahman, S.S. 2000. An experimental investigation of hydraulic behaviour of fractures and joints in granitic rock. *International Journal of Rock Mechanics & Mining Sciences* **37**: 1061-1071.

Cox, D.O., Kuuskraa, V.A., and Hansen, J.T. 1996. Advanced Type Curve Analysis for Low Permeability Gas Reservoirs. Paper SPE 35595 presented at the 1996 Gas Technology Conference, Calgary, Alberta, Canada, 28 April – 1 May. doi: 10.2118/35595-MS.

Dyke, C.G., Wu, B., and Milton-Tayler, D. 1995. Advances in Characterizing Natural-Fracture Permeability From Mud-Log Data. *SPE Formation Evaluation* **10** (3): 160-166. SPE 25022-PA. doi: 10.2118/25022-PA.

Erlend, H.V., Nygaard, G., Lorentzen, R.J., and Fjelde, K.K. 2003. Reservoir Characterization during UBD: Methodology and Active Tests. Paper IADC/SPE 81634 presented at the IADC/SPE Underbalanced Technology Conference and Exhibition, Houston, Texas, USA, 25-26 March. doi: 10.2118/81634-MS.

Fetkovich, M.J. 1980. Decline Curve Analysis Using Type Curves. *JPT* (June 1980) 1066-1077.

Friedel, T., Mtchedlishvili, G., Voigt, H.-D., and Hafner, F. 2008. Simulation of Inflow While Underbalanced Drilling With Automatic Identification of Formation Parameters and Assessment of Uncertainty. *SPE Res Eval & Eng* **11** (2): 292-297. SPE 93974-PA. doi: 10.2118/93974-PA.

Gale, J.F.W., Reed, R.M., and Holder, J. 2007. Natural fractures in the Barnett Shale and their importance for hydraulic fracture treatments. AAPG Bulletin 91 (4) (April 2007): 603-622.

Gaskari, R., Mohaghegh, S.D., and Jalali, J. 2006. An Integrated Technique for Production Data Analysis with Application to Mature Fields. Paper SPE 100562 presented at the 2006 SPE Gas Technology Symposium, Calgary, Alberta, Canada, 15-17 May. doi: 10.2118/100562-MS.

Gaskari, R., Mohaghegh, S.D., and Jalali, J. 2007. An Integrated Technique for Production Data Analysis (PDA) With Application to Mature Fields. *SPE Prod & Oper (*November 2007) 403-416.

Geosearch Logging Inc. "Wellsite Geology and Gas Detection." Accessed October 20, 2011. http://www.geosearchlogging.com/employee/HydrocarbonWellLoggingHandout.pdf.

Gonzalez, M.H., Bukacek, R.F., and Lee, A.L. 1967. The Viscosity of Methane. SPE Journal 7 (1): 75-79. SPE 1483-PA. doi: 10.2118/1483-PA.

Huang, J., Griffiths, D.V., and Wong, S.-W. 2010. Characterizing Natural Fracture Permeability from Mud Loss Data. Accepted for publication in the *SPE Drilling and Completion* (submitted 2010).

Hunt, J.L., and Rester, S. 2000. Reservoir Characterization During Underbalanced Drilling: A New Model. SPE 59743 presented at the 2000 SPE/CERI Gas Technology Symposium, Calgary, Alberta, Canada, 3-5 April. doi: 10.2118/59743-MS.

Kalathingal, P., and Kuchinski, R. 2010. The Role of Resistivity Image Logs in Deep Natural Gas Reservoirs. Paper SPE 131721 presented at the SPE Deep Gas Conference and Exhibition, Manama, Bahrain, 24-26 January 2010. doi: 10.2118/131721-MS.

Kardolus, C.B., and van Kruijsdijk, C.P.J.W. 1997. Formation Testing While Underbalanced Drilling. Paper SPE 38754 presented at the 1997 SPE Annual Technical Conference and Exhibition, San Antonio, Texas, USA, 5-8 October. doi: 10.2118/38754-MS.

King, G.E. 2010. Thirty Years of Gas Shale Fracturing: What Have We Learned? Paper SPE 133456 presented at the 2010 SPE Annual Technical Conference and Exhibition, Florence, Italy, 19-22 September. doi: 10.2118/133456-MS.

Kneissl, W. 2001. Reservoir Characterization Whilst Underbalanced Drilling. Paper SPE/IADC 67690 presented at the SPE/IADC Drilling Conference, Amsterdam, The Netherlands, 27 February – 1 March. doi: 10.2118/67690-MS.

Kubik, W., and Lowry, P. 1993. Fracture Identification and Characterization Using Cores, FMS, CAST, and Borehole Camera: Devonian Shale, Pike County, Kentucky. Paper SPE 25897 presented at the 1993 SPE Rocky Mountain Regional/Low Permeability Reservoirs Symposium, Denver, CO, USA, 12-14 April. Doi: 10.2118/25897-MS.

Larsen, L., and Nilsen, F. 1999. Inflow Predictions and Testing While Underbalanced Drilling. Paper SPE 56684 presented at the 1999 SPE Annual Technical Conference and Exhibition, Houston, Texas, USA, 3-6 October. doi: 10.2118/56684-MS.

Lavrov, A., and Tronvoll, J. 2004. Modeling Mud Loss in Fractured Formations. Paper 88700 presented at the 2004 11th Abu Dhabi International Petroleum Exhibition and Conference, Abu Dhabi, U.A.E., 10-13 October. doi: 10.2118/88700-MS.

Lee, W.J., and Wattenbarger, R.A. 1996. *Gas Reservoir Engineering.* SPE Textbook Series.

Liétard, O., Unwin, T., Guillot, D.J., and Hodder, M.H. 1999. Fracture Width Logging While Drilling and Drilling Mud/Loss-Circulation-Material Selection Guidelines in Naturally Fractured Reservoirs. *SPE Drilling and Completion* **14** (3): 168-177. SPE 57713-PA. doi: 10.2118/57713-PA.

Majidi, R., Miska, S.Z., Yu, M., and Thompson, L.G. 2008a. Quantitative Analysis of Mud Losses in Naturally Fractured Reservoirs: The Effect of Rheology. Paper SPE 114130 presented at the 2008 Western Regional and Pacific Section AAPG Joint Meeting, Bakersfield, California, USA, 31 March – 2 April. doi: 10.2118/114130-MS.

Majidi, R., Miska, S.Z., Yu, M., and Thompson, L.G. 2008b. Modeling of Drillilng Fluid Losses in Naturally Fractured Formations. Paper SPE 114630 presented at the 2008 SPE Annual Technical Conference and Exhibition, Denver, Colorado, USA, 21-24 September. doi: 10.2118/114630-MS.

McLean, K., and McNamara, D. 2010. Fractures Interpreted From Acoustic Formation Imaging Technology: Correlation to Permeability. Proceedings, Thirty-Sixth Workshop on Geothermal Reservoir Engineering, California, USA, 31 January – 2 February 2011. SGP-TR-191.

Millheim, K.K., and Cichowicz, L. 1968. Testing and Analyzing Low-Permeability Fractured Gas Wells. *J Pet Technol* (February 1968) 193-198.

Mercer, R.F. 1974. Liberated, Produced, Recycled or Contamination. SPWLA 15th Annual Logging Symposium, 2-5 June, 1974.

Moore, M.C. 2010. Policy and Regulation in the Face of Uncertainty: The Case of Disruptive Markets for Unconventional Natural Gas in North America. Paper CSUG/SPE 138167 presented at the Canadian Unconventional Resources & International Petroleum Conference, Calgary, Alberta, Canada, 19-21 October 2010. doi: 10.2118/138167-MS.

Mourzenko, V.V., Thovert, J.F., and Adler, P.M. 1995. Permeability of a Single Fracture; Validity of the Reynolds Equation. *J. Phys. II France* **5** (March 1995) 465-482.

Myal, F.R., and Frohne, K-H. 1992. Drilling and Early Testing of a Sidetrack to the Slant-Hole Completion Test Well: A Case Study of Gas Recovery Research in Colorado's Piceance Basin. Papter SPE 24382 presented at the SPE Rocky Mountain Regional Meeting, Casper, Wyoming, USA, 18-21 May 1992. doi: 10.2118/24382-MS.

Ramalho, J. 2006. Underbalanced Drilling In The Reservoir, An Integrated Technology Approach. Paper SPE 103576 presented at the 2006 SPE Russian Oil and Gas Technical Conference and Exhibition, Moscow, Russia, 3-6 October. doi: 10.2118/103576-MS.

Ramalho, J., Elliott, D., Francis, P., and Medeiros, R.S. 2009. Tight Gas Reservoir Exploitation With Underbalanced Drilling Technology. Paper IPTC 14109 presented at the 2009 International Petroleum Technology Conference, Doha, Qatar, 7-9 December. doi: 10.2523/14109-MS.

Sanfillippo, F., Brignoli, M., Santarelli, F.J., and Bezzola, C. 1997. Characterization of Conductive Fractures While Drilling. Paper SPE 38177 presented at the 1997 SPE European Formation Damage Conference, The Hague, The Netherlands, 2-3 June. doi: 10.2118/38177-MS.

Snow, D.T. A Parallel Plate Model of Fractured Permeable Media (PhD diss., University of California, Berkeley, 1965).

Stewart, P.R. 1970. Low-Permeability Gas Well Performance At Constant Pressure. *J Pet Technol* (September 1970) 1149-1156.

Vairogs, J., Hearn, C.L., Dareing, D.W., and Rhoades, V.W. 1971. Effect of Rock Stress on Gas Production From Low-Permeability Reservoirs. *J Pet Technol* (September 1971) 1161-1167.

Verga, F.M., Carugo, C., Chelini, V., Maglione, R., and De Bacco, G. 2000. Detection and Characterization of Fractures in Naturally Fractured Reservoirs. Paper SPE 63266 presented at the 2000 Annual Technical Conference and Exhibition, Dallas, Texas, USA, 1-4 October. doi: 10.2118/63266-MS.

Wang, Z., Peden, J.M., and Lemanczyk, R.Z. 1994. Gas Kick Simulation Study for Horizontal Wells. Paper IADC/SPE 27498 presented at the 1994 IADC/SPE Drilling Conference, Dallas, Texax, USA, 15-18 February. doi: 10.2118/27498-MS.

Warren, J.E., and Root, P.J. 1963. The Behavior of Naturally Fractured Reservoirs. *SPE Journal* **3** (3): 245-255. SPE 426-PA. doi: 10.2118/426-PA.

Wattenbarger, R.A., El-Banbi, A.H., Villegas, M.E., and Maggard, J.B. 1998. Production Analysis of Linear Flow Into Fractured Tight Gas Wells. Paper SPE 39931 presented at the 1998 SPE Rocky Mountain Regional/Low-Permeability Reservoirs Symposium and Exhibition, Denver, Colorado, USA, 5-8 April. doi: 10.2118/39931-MS.

Wei, Y., and Economides, M.J. 2005. Transverse Hydraulic Fractures From a Horizontal Well. Paper SPE 94671 presented at the 2005 SPE Annual Technical Conference and Exhibition, Dallas, Texas, USA, 9-12 October. doi: 10.2118/94671-MS.

Witherspoon, P.A., Wang, J.S.Y., Iwai, K., and Gale, J.E. 1980. Validity of Cubic Law for Fluid Flow in a Deformable Rock Fracture. *Water Resources Research* **16** (6) 1016-1024.

Woodrow, C.K., Elliott, D., Pickles, R., and Weatherford, D.B. 2008. One Company's First Exploration UBD Well for Characterizing Low Permeability Reservoirs. Paper SPE 112907 presented at the 2008 SPE North Africa Technical Conference and Exhibition, Marrakech, Morocco, 12-14 March. doi: 10.2118/112907-MS.

Wu, Y-S., personal communication, June 2011.

Xiong, H. and Holditch, S.A. 2006. Will the Blossom of Unconventional Natural Gas Development in North America Be Repeated in China? Paper SPE 103775 presented at the 2006 SPE International Oil & Gas Conference and Exhibition, Beijing, China, 5-7 December. doi: 10.2118/103775-MS.

Zeng, F., and Zhao, G. 2010. The optimal hydraulic fracture geometry under non-Darcy flow effects. *Journal of Petroleum Science and Engineering* **72** (2010) 143-157.

APPENDIX A: CONTENTS OF THE CD

Please see accompanying CD for a copy of the user's manual for the computational program, the Excel spreadsheet template used for input and output, and a copy of the code for the computational program.